Integrated photonics incorporating 2D materials designed for industrial and commercial applications

David Moss

▶ **To cite this version:**

David Moss. Integrated photonics incorporating 2D materials designed for industrial and commercial applications. 2025. hal-04924706

HAL Id: hal-04924706
https://hal.science/hal-04924706v1

Preprint submitted on 31 Jan 2025

HAL is a multi-disciplinary open access archive for the deposit and dissemination of scientific research documents, whether they are published or not. The documents may come from teaching and research institutions in France or abroad, or from public or private research centers.

L'archive ouverte pluridisciplinaire **HAL**, est destinée au dépôt et à la diffusion de documents scientifiques de niveau recherche, publiés ou non, émanant des établissements d'enseignement et de recherche français ou étrangers, des laboratoires publics ou privés.

Distributed under a Creative Commons Attribution 4.0 International License

Integrated photonics incorporating 2D materials designed for industrial and commercial applications

David J. Moss

Optical Sciences Centre, Swinburne University of Technology, Hawthorn, VIC 3122, Australia

Email: dmoss@swin.edu.au

Keywords: Integrated Photonics, 2D materials, nanophotonics

ABSTRACT

On-chip integration of 2D materials with exceptional optical properties provides an attractive solution for next-generation photonic integrated circuits to address the limitations of conventional bulk integrated platforms. Over the past two decades, significant advancements have been made in the interdisciplinary field of 2D material integrated photonics, greatly narrowing the gap between laboratory research and industrial applications. In this paper, we provide a perspective on the developments of this field towards industrial manufacturing and commercialization. First, we review recent progress towards commercialization. Next, we provide an overview of cutting-edge fabrication techniques, which are categorized into large-scale integration, precise patterning, dynamic tuning, and device packaging. Both the advantages and limitations of these techniques are discussed in relation to industrial manufacturing. Finally, we highlight some important issues related to commercialization, including fabrication standards, recycling, service life, and environmental implications.

I. INTRODUCTION

Integrated circuits (ICs) have been the driving force behind the information age. Since the first demonstration of a prototype IC in 1958 by Nobel laureate Jack Kilby,[1] many technological breakthroughs have rapidly advanced their development, continually improving their core benefits including compact footprint, low power consumption, high scalability, and cost-effective mass production. After more than 60

years of development, ICs have now become a cornerstone of modern industry, driving revolutionary changes worldwide and profoundly impacting people's lives.

In modern IC industry, the complementary metal-oxide-semiconductor (CMOS) fabrication is a dominant manufacturing technology with well-established production lines and fabrication standards.[2, 3] By leveraging the well-developed CMOS fabrication technology, photonic integrated circuits (PICs) not only reap the dividends of electronic ICs with respect to the device footprint, energy consumption, and mass producibility, but also provide additional benefits such as large processing bandwidth, strong immunity to electromagnetic interference, and capability for massively parallel processing.[4-6] These make them competitive for overcoming the intrinsic bandwidth bottleneck of electronic ICs in many high-bandwidth applications.[7, 8]

As the CMOS technology continues to push the boundaries of device miniaturization, the inherent limitations in material properties of conventional PICs pose challenges in meeting the ever-increasing demands for device functionality and performance.[9] For example, as a dominant integrated material platform, silicon's indirect bandgap hinders its use in laser applications.[10] In addition, the strong two-photon absorption in silicon at the near-infrared wavelengths greatly limits its effectiveness in many nonlinear optical applications.[11]

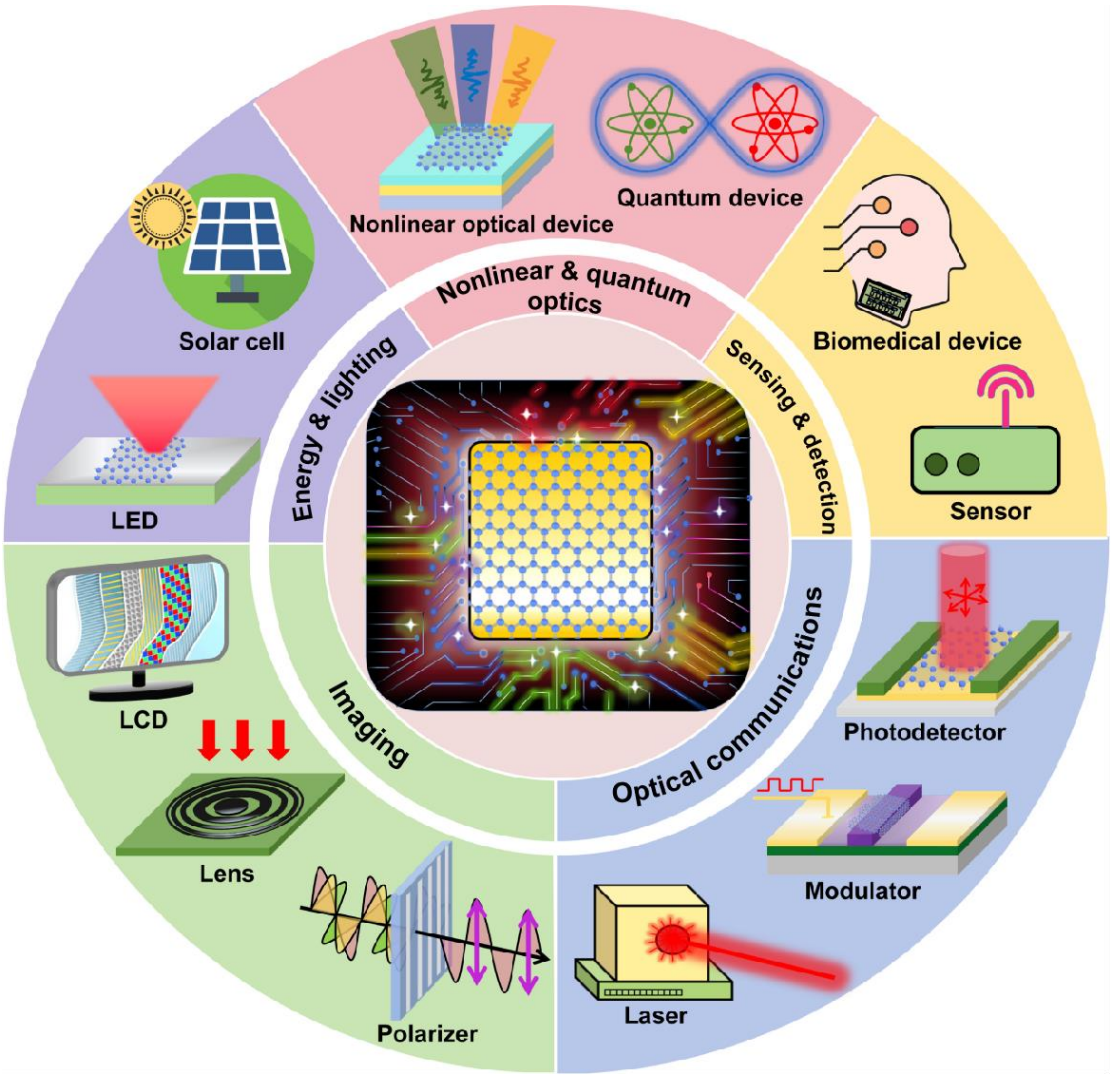

FIG.1. Diverse applications of integrated photonic devices incorporating 2D materials. LCD: liquid crystal display. LED: light emitting diode

On-chip integration of other functional materials with superior properties has proven to be a promising solution to address the limitations of conventional PICs. Since the first isolation of graphene in 2004,[12] atomically thin two-dimensional (2D) materials have received enormous interests, with a fast-growing family including transition metal dichalcogenides (TMDCs), graphene oxide (GO), black phosphorus (BP), hexagonal boron nitride (hBN), and many others. Unlike their bulk counterparts, 2D materials demonstrate a range of exceptional properties, such as ultrahigh carrier mobility, broadband optical response, layer-dependent optical bandgaps, significant material anisotropy, and high optical nonlinearity.[13-18] Moreover, unlike the common lattice mismatch issue faced with bulk integrated materials, 2D materials are feature by dangling-bond free surface and an inherent propensity to adhered through van der

Waals.[19,20] This allows for stress-free on-chip integration and provides a high flexibility in device design.

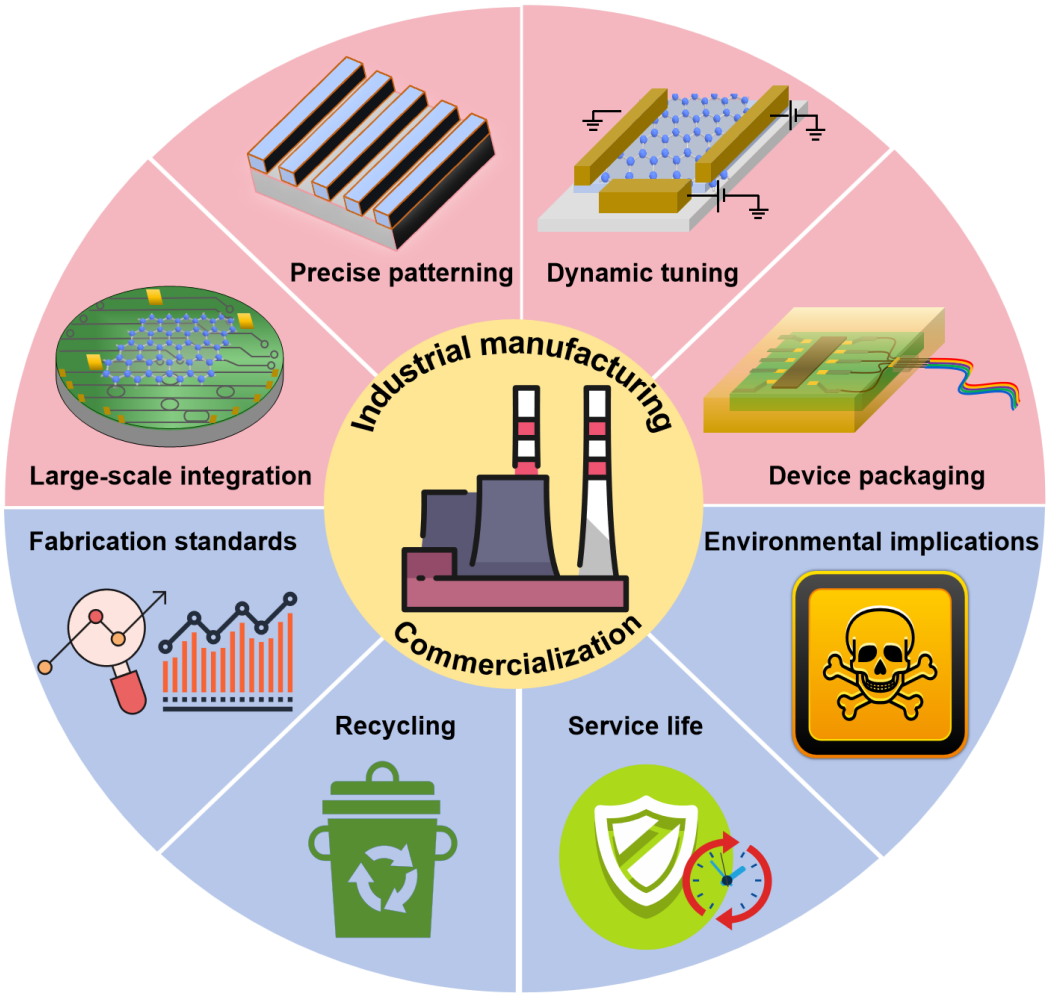

FIG.2. Key requirements for industrial manufacturing and commercialization of integrated photonic devices incorporating 2D materials.

Over the past two decades, significant progress has been made in the interdisciplinary field of 2D material integrated photonics. A number of integrated photonic devices incorporating 2D materials have demonstrated new functionalities and improved performance that surpass what the conventional bulk integrated photonic devices can offer,[21-28] covering a wide range of applications as summarized in **Fig. 1**. The huge progress in 2D material integrated photonics is not only intriguing for laboratory research but also paves the way for many industrial applications.

In this paper, we provide a perspective on the development of 2D material integrated photonics, with a particular focus on its trajectory towards industrial

manufacturing and commercialization. We review the current progress, discuss future opportunities, and highlight the remaining gap between the two. The structure of this perspective is illustrated in **Fig. 2**. First, we review recent progress towards commercialization of integrated photonic devices incorporating 2D materials. Next, we provide an overview of cutting-edge fabrication techniques, which are categorized into large-scale integration, precise patterning, dynamic tuning, and device packaging. We discuss both their merits and limitations in the context of industrial manufacturing. Finally, we discuss some critical issues related to commercialization, including fabrication standards, recycling, service life, and environmental implications.

II. COMMERCIALIZATION PROGRESS

Since the ground-breaking work on isolation of graphene in 2004, 2D materials have become a highly active research area over the past two decades, as evidenced by a wealth of related publications and patents. Along with extensive research on these atomically thin materials, there has also been growing interest in the pursuit of 2D materials in commercial products. In the past decade, exciting progress has been made in bridging laboratory research to industrial manufacturing. This section provides an overview of these advancements in integrated photonic devices incorporating 2D materials.

Fig. 3 shows some examples of state-of-the-art hybrid integrated photonic devices with 2D materials, including both commercially available products and laboratory-successful devices with a high level of market readiness. **Fig. 3(a)** shows a 10-Gb/s integrated graphene phase modulator demonstrated by an international team led by the Photonic Networks and Technologies National Laboratory in Italy.[29] By integrating the graphene phase modulator into a Mach-Zehnder interferometer configuration, a static modulation depth of ~35 dB and a modulation efficiency of ~0.28 V·cm was achieved, which outperform silicon-based PN junctions and comparable to modulators based on silicon-insulator-silicon capacitors. **Fig. 3(b)** shows a commercially available graphene photodetector from the Emberion corporation.[30] By integrating graphene and nanostructured optical absorbers with specially designed read-out circuits, it was

capable of detecting light across a wide wavelength range of ~400 – 1800 nm. **Fig. 3(c)** shows a graphene optoelectronic mixer demonstrated by the Thales Research and Technology in collaboration with the University of Lille and IEMN and the University of Cambridge.[31] It achieved an operation bandwidth of ~20 GHz, with a conversion efficiency surpassing those of previous graphene mixers by more than two orders of magnitude.

Fig. 3(d) shows a high-efficient perovskite solar cell designed by the Swift Solar corporation.[32] By combining metal halide perovskites with silicon substrates, this tandem solar cell was able to surpass the 30% conversion efficiency barrier that limited traditional solar cells. **Fig. 3(e)** shows a graphene-GaN light-emitting diode (LED) demonstrated by the Gwangju Institute of Science and Technology in Korea.[33] It achieved a sheet resistance of ~620 ohms per square and a transparency exceeding 85% in the 400 – 800 nm wavelength range, outperforming conventional GaN LEDs with indium tin oxide. **Fig. 3(f)** shows GO hologram demonstrated by researchers from the University of Shanghai for Science and Technology.[34] The hologram image was patterned via direct laser writing and was able to be erased via oxygen plasma treatment, providing a facile, low-cost, and rewritable method for hologram imaging.

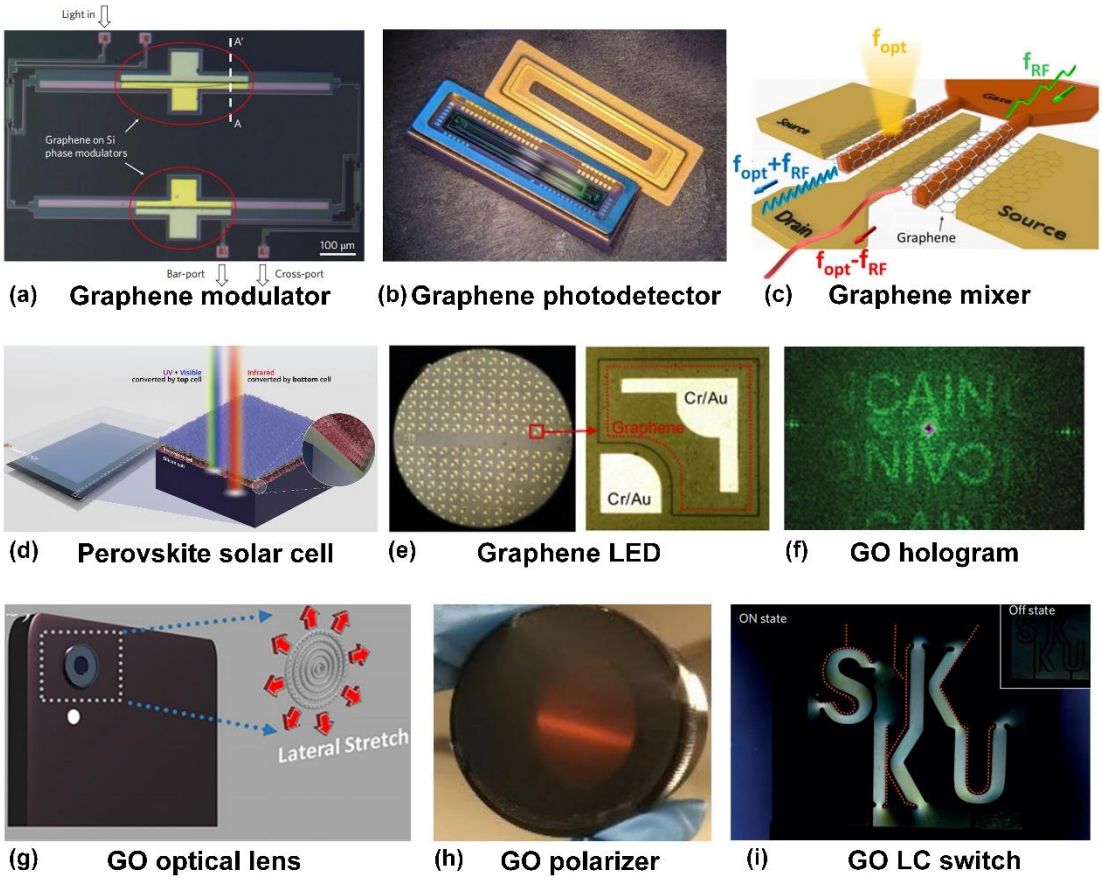

FIG. 3. Commercialization of integrated photonic devices incorporating 2D materials. (a) A graphene phase modulator from the Photonic Networks and Technologies National Laboratory in Italy. (b) A graphene photodetector from the Emberion corporation. (c) A graphene optoelectronic mixer demonstrated by the Thales Research and Technology in collaboration with the University of Lille and IEMN and the University of Cambridge. (d) A perovskite solar cell from the Swift Solar corporation. (e) A graphene-GaN light-emitting diode (LED) demonstrated by researchers from the Gwangju Institute of Science and Technology. (f) GO hologram demonstrated by researchers from the University of Shanghai for Science and Technology. (g) A GO optical lens demonstrated by researchers from Shenzhen University and Swinburne University of Technology. (h) A GO optical polarizer demonstrated by researchers from Swinburne University of Technology. (i) A GO liquid-crystal (LC) switch demonstrated by researchers from Sungkyunkwan University. (a) Reproduced with permission from Sorianello *et al.*, Nat. Photonics **12**(1), 40-44 (2017). Copyright 2017 Springer Nature. (b) Reproduced from https://optics.org/news/10/6/18. (c) Reproduced with permission from Montanaro *et al.*, Nat. Commun. **12**(1), 2728 (2021). Copyright 2021 Springer Nature. (d) Reproduced from https://www.swiftsolar.com/tech/. (e) Reproduced with permission from Jo *et al.*, Nanotechnology **21**(17), 175201 (2010). Copyright 2010 IOP Publishing. (f) Reproduced with permission from Wan *et al.*, Adv. Opt. Mater. **11**(22), 2300872 (2023). Copyright 2023 John Wiley and Sons. (g) Reproduced with permission from Wei *et al.*, ACS Nano **15**(3), 4769-4776 (2021). Copyright 2021 American Chemical Society. (h) Reproduced with permission from Zheng *et al.*, Nanoscale **12**(21), 11480-11488 (2020). Copyright 2020 RSC Pub. (i) Reproduced with permission from Shen *et al.*, Nat. Mater. **13**(4), 394-9 (2014). Copyright 2014 Springer Nature.

Fig. 3(g) shows a GO optical lens demonstrated by researchers from Shenzhen University and Swinburne University of Technology.[35] The ultrathin lens, with a thickness of ~250 nm, enabled color imaging and simultaneous focal length tunability across the entire visible spectrum. By laterally stretching the lens, it achieved over 20% focal length tuning, surpassing traditional lenses that rely on tuning the distance between multiple optical elements. **Fig. 3(h)** shows a GO optical polarizer (mounted on a commercial standard polarizer mount) demonstrated by researchers from Swinburne University of Technology.[36] This device achieved a high polarization extinction ratio of ~ 20 dB, along with adjustable operation wavelengths in the mid-infrared region. **Fig. 3(i)** shows a GO-liquid crystal (LC) switch demonstrated by Sungkyunkwan University, [37] achieving 15:1 contrast between the on and off states under an applied voltage of ~20 V. The large polarizability anisotropy of GO also yielded a large Kerr coefficient that was about three orders of magnitude higher than that for molecular LCs.

Now the research on 2D materials is at a stage where most of outstanding properties of conventional 2D materials such as graphene, GO, TMDC, hBN have already been studied, and the focus is gradually shifting towards industrial-scale production and the development of commercial products for these materials. In the past decade, there has been a surge of related commercial activities, with efforts focused on bringing relevant products to market. For instance, the Graphene Flagship initiative, which brings together 118 academic and industrial partners, launched projects such as METROGRAPH, GBIRCAM, AUTOVISION, and GRAPES to explore graphene-based devices for displays, imaging technologies, and solar cells.[38] The INNOFOCUS corporation seeks to leverage 2D materials with innovative nanostructures to develop advanced photonic devices, catering to industrial requirements across various applications.[39] On the other hand, studies on a range of new 2D materials, such as MXenes, metal-organic frameworks (MOFs), and ferroelectric materials, continue to emerge and reveal intriguing properties. However, most of them remain for laboratory research, with commercialization still in infancy and yet to be developed. In the future, closer collaboration between academia and industry is anticipated, with increased focus on improving fabrication techniques and product quality, to facilitate more rapid

progress toward industrial manufacturing and commercialization of related products.

III. FABRICATION TECHENIQUES

Over the past two decades, alongside the surge in activities related to 2D materials, many related fabrication techniques have been developed, demonstrating great potential for large-scale industrial manufacturing. In this section, we present an overview of cutting-edge techniques for fabricating integrated photonic devices incorporating 2D materials, highlighting their potential and limitations in industrial manufacturing. It is divided into four parts, including large-scale integration, precise patterning, dynamic tuning, and device packaging.

A. Large-scale integration

Producing high-quality integrated wafers, such as the silicon-on-insulator (SOI) wafers, is the initial step in manufacturing integrated photonic devices. Current fabrication techniques, such as chemical vapor deposition (CVD) and physical vapor deposition (PVD), have already enabled industrial-scale manufacturing of high-quality integrated wafers in different sizes (*e.g.*, 4, 8, and 12 inches).[40-42] In this part, we focus on discussing methods for integration of 2D materials onto these wafers. To achieve this, the process typically involves two steps: synthesizing 2D materials and transferring them onto integrated substrates. In some cases, 2D materials can be directly synthesized on integrated wafers, thus simplifying the overall process.

Synthesizing high-quality 2D materials is essential for implementing hybrid devices with high performance. Mechanical exfoliation, liquid-phase exfoliation (LPE), and chemical vapor deposition (CVD) are three main methods for synthesizing 2D materials. Mechanical exfoliation provides a simple and efficient way to synthesize 2D materials without using complex facilities. However, for large-scale industrial fabrication, it suffers from limitations due to the inconsistent thicknesses and small sizes of the 2D flakes produced by this method. LPE is a solution-based method to synthesize 2D materials, allowing for cost-effective production of large volumes of 2D nanoflakes. Similar to mechanical exfoliation, it also faces limitations induced by small

sizes of the exfoliated 2D flakes. In contrast to the above exfoliation methods, CVD offers an attractive approach for growing high-quality 2D films over large areas with precise thickness control. This makes it appealing for industrial production of high-quality 2D films. Despite this, the state-of-the-art CVD method for synthesizing 2D materials still faces challenges such as limited efficiency, film contamination, and complex process control.

In addition to the above three main methods, some other methods for synthesizing 2D materials have also been investigated, such as molecular beam epitaxy (MBE)[43, 44] and PVD.[45, 46] MBE is a precise atomic layer by layer growth technique used to grow single crystal films epitaxially on an existing crystal substrate. It was invented for the growth of compound semiconductors in the 1970s and has been successfully applied to the growth of metals, oxides, and topological materials.[47] Recently, this technique has also been employed to grow high-quality monolayer graphene, TMDCs, and h-BN.[48-50] The main limitation of current MBE technique is that it requires significantly higher vacuum levels than other deposition methods to achieve comparable impurity levels in the grown films.[51, 52] The PVD method involves a process where material transitions from a condensed phase to a vapor phase, and then recondenses into a thin film. Sputtering and evaporation are two widely used PVD techniques for coating thin films of metal, glass, and polymers in industrial manufacturing. Recently, the PVD method has been employed for fabricating thin hBN, MXenes, and perovskite films. Compared to CVD and MBE, it provides higher deposition rates, but this comes with the trade-off of larger 2D film thicknesses (typically > 30 nm).[45, 46, 53]

After synthesizing 2D materials, it is usually needed to transfer them onto the target integrated substrates to construct hybrid devices. Dry transfer methods using transfer stamps[54] was widely employed for transferring mechanically exfoliated 2D flakes in the early research of this field.[12, 55-57] However, several factors restrict the applicability of this method to laboratory environments instead of industrial production. These mainly include challenges in processing flakes with large lateral size, low fabrication yield, and reliance on complicated supporting facilities. For 2D flakes synthesized by LPE, solution dropping techniques such as drop casting, spin and spray

coating are commonly used for their on-chip transfer.[58, 59] Although these methods provide a fast way to prepare 2D films over large areas, they face limitations such as low film uniformity (typically > 10 nm[60]) and large film thicknesses (typically > 100 nm[61]), restricting its use for fabricating films with low thicknesses.

For 2D films synthesized by the CVD method, a high growth temperature is usually needed. As a result, they are typically deposited on metal substrates or foils, rather than dielectric substrates used for integrated photonic devices (*e.g.*, silicon, silicon nitride, silica). Consequently, subsequent film transfer processes are required. Unlike the dry transfer techniques, which are commonly used for small exfoliated 2D flakes, wet transfer techniques are typically employed for transferring CVD-grown 2D films with large lateral sizes.[62, 63] They are easier to operate and do not require sophisticated facilities, resulting in higher success rates and improved transfer efficiency than the dry transfer techniques. Despite these advantages, problems like stretching, wrinkling, and bending can easily occur during the on-chip transfer process, even though CVD-grown 2D films can achieve a high uniformity on the original substrates. This makes it challenging to achieve highly uniform coating or conformal coating on integrated waveguides and metasurfaces, potentially impairing device performance in some applications.[64]

In recent years, several representative works have been reported to address the limitations of the previously mentioned transfer techniques, as summarized in **Fig. 4**. In **Fig. 4(a)**, success transfer of CVD-grown graphene films onto 4-inch silica/silicon wafers was achieved by introducing a transfer medium polymer (polyvinyl alcohol mixed with sorbitol molecules),[65] where the adhesion between the polymer and graphene layers was adjusted through freezing-induced crosslinking, enabling crack-free film transfer over large areas. In **Fig. 4(b)**, a modified solution dropping method was demonstrated by using electrochemical intercalation to prepare high-quality molybdenum disulfide (MoS_2) solutions,[66] which allowed the coating of large-area MoS_2 films with low thicknesses (~3.6 nm) and high uniformity. In **Fig. 4(c)**, a new solution-based film coating method relying on self-assembly of GO monolayers was demonstrated.[67] This method enabled not only layer-by-layer film coating over large

areas on dielectric substrates like silicon, silicon nitride, and silica,[68, 69] but also conformal coatings on integrated waveguides and metasurfaces.[28, 70]

In **Fig. 4(d)**, a tri-layer transfer medium (polymethyl methacrylate (PMMA)/Borneol/graphene) with gradient surface energy was employed to improve the wet transfer process, allowing reliable adhesion to and release from the target substrates.[71] In **Fig. 4(e)**, to maintain 2D films with flat, intact and clean surfaces during the transfer process, supporting films were introduced by incorporating oxhydryl groups-containing volatile molecules into PMMA.[72] These films could deform under heat, thus enabling controllable conformal contact with different 2D films such as graphene and MoS_2. In **Fig. 4(f)**, a modified CVD method, combined with a bubble transfer method, was developed to fabricate a 30 × 30 mm single crystal hBN film on a silica/silicon wafer.[73] During the fabrication process, the hBN was delaminated from liquid Au substrates by using hydrogen bubbles generated by electrolysis. This enables the fabrication of high-quality hBN films free from grain boundaries that significantly influence the film uniformity and mechanical strength.

By combining the precise positioning of dry transfer techniques and the high efficiency of wet transfer techniques, a hybrid technique called semi-dry transfer has been developed. For instance, in **Fig. 4(g),** three large graphene sheets of up to 50 × 50 mm^2 were transferred to a silicon wafer with over 99% yield.[74] This was achieved by using functional tapes with their adhesive forces controlled by ultraviolet light, along with electrochemical delamination. In **Fig. 4(h)**, the semi-dry transfer method was employed to fabricate a monolayer tungsten disulfide (WS_2) on a silicon wafer. During the transfer process, the film was first exfoliated by thermal release tape assisted with a Ni film, followed by releasing the tape/Ni/film on the target wafer. Subsequently, the tape was removed by annealing, and the Ni was etched away using $FeCl_3$.[75] In **Fig. 4(i)**, direct growth of monolayer MoS_2 films onto 12-inch silicon wafers was achieved by pre-positioning amorphous Al_2O_3 films as interlayers. This provides an effective way for in-situ growing 2D films onto integrated wafers without the film transfer process.[76]

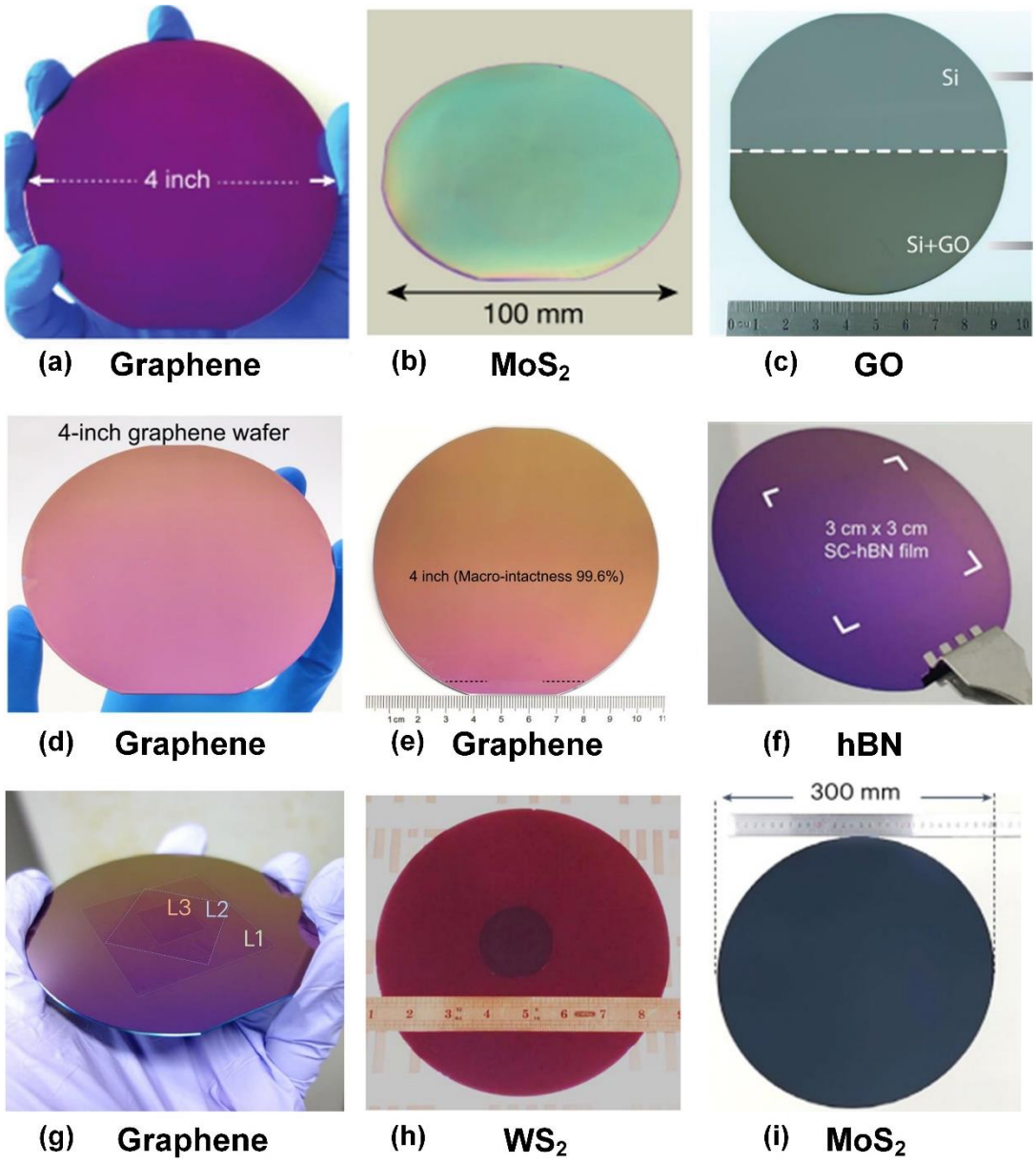

FIG. 4. Wafer-scale integrated 2D material films. (a) A graphene film integrated on a 4-inch silicon wafer via dry transfer method. (b) A MoS_2 film integrated on a 100-mm diameter silicon wafer via solution dropping method. (c) A GO film integrated on a 4-inch silicon wafer via self-assembly method. (d) A graphene film integrated on a 4-inch silicon wafer via wet transfer method. (e) A graphene film integrated on a 4-inch silicon wafer via bubbling-based wet transfer method. (f) An hBN film integrated on a silicon wafer via wet transfer method. (g) A graphene film integrated on a silica substrate via semi-dry transfer method. (h) A WS_2 film integrated on an 8-inch silicon wafer via semi-dry transfer method. (i) A MoS_2 film integrated on a 12-inch silicon wafer via direct growth method. (a) Reproduced with permission from Chen *et al.*, Adv. Mater. **36**(15), e2308950 (2024). Copyright 2024 John Wiley and Sons. (b) Reproduced with permission from Lin *et al.*, Nature **562**(7726), 254-258 (2018). Copyright 2018 Springer Nature. (c) Reproduced with permission from Yang *et al.*, ACS Photonics **6**(4), 1033-1040 (2019). Copyright 2019 American Chemical Society. (d) Reproduced with permission from Gao *et al.*, Nat. Commun. **13**(1), 5410 (2022). Copyright 2022 Springer Nature.

(e) Reproduced with permission from Zhao *et al*., Nat. Commun. **13**(1), 4409 (2022). Copyright 2022 Springer Nature. (f) Reproduced with permission from Lee *et al*., Science **362**(6416), 817-821 (2018). Copyright 2018 The American Association for the Advancement of Science. (g) Reproduced with permission from Nakatani *et al*., Nat. Electron. **7**, 119-130 (2024). Copyright 2024 Springer Nature. (h) Reproduced with permission from Shim *et al*., Science **362**(6415), 665-670 (2018). Copyright 2018 The American Association for the Advancement of Science. (i) Reproduced with permission from Xia *et al*., Nat. Mater. **22**(11), 5410 (2023). Copyright 2023 Springer Nature.

Tabel I summarizes several synthesis and transfer techniques with high potential for large-scale manufacturing (some of which were discussed in **Fig. 4**), along with the relevant publications that utilize these methods. Although the current methods represent significant progress toward industrial manufacturing, challenges still remain. The modified dry transfer method in **Fig. 4(a)** has difficulties in achieving high fabrication yield and accurate film thickness control. The modified solution dropping method in **Fig. 4(b)** has limitations related to reproducibility and solution contamination. The self-assembly method in **Fig. 4(c)** face challenges for fabricating thick (>200 nm) films due to its time-consuming nature, as well as increased scattering loss in thicker films. The performance of the modified wet transfer techniques in **Figs. 4(d) − (f)** can be compromised by challenges such as residual solvents induced by the chemical solution, precise alignment during the transfer, and variability in thickness control. The semi-dry transfer approaches in **Figs. 4(g)** and **4(h)** are currently limited by the complexity of the transfer procedures and potential contamination from chemical solutions. The introduction of Al_2O_3 interlayers for the direct growth method in **Fig. 4(i)** was used for fabricating TMDCs, and its applicability to other 2D materials remains to be investigated. In the future, fabrication techniques for large-scale integration of 2D materials can be further developed on the basis of these methods, along with the introduction of new techniques, to ultimately achieve the goal of industrial manufacturing.

TABLE I. Synthesis and transfer techniques with high potential for on-chip integration of 2D materials in industrial manufacturing. CVD: chemical vapor deposition, LPE: liquid-phase exfoliation.

2D Materials	2D film thickness	Integrated substrate	Synthesis method	Transfer method	Ref.
Graphene	Monolayer	4-inch silicon wafer	CVD	Dry transfer	[65]
Graphene	Monolayer	4-inch silicon wafer	CVD	Wet transfer	[71]
Graphene	~1.6 nm	4-inch silicon wafer	CVD	Wet transfer	[72]
Graphene	Monolayer	silicon wafer	CVD	Semi-dry transfer	[74]
GO	~ 2 μm	SU-8 polymer	LPE	Drop casting	[77]
GO	~1 nm	4-inch silicon wafer	LPE	Self-assembly	[67]
MoS_2	~0.8 nm	6-inch silicon wafer	CVD	Wet transfer	[78]
MoS_2	~3.8 nm	100-mm diameter silicon wafer	LPE	Spin coating	[66]
MoS_2	10.5 − 11.4 nm	2-inch silicon wafer	LPE	Spin coating	[79]
MoS_2	Monolayer	12-inch silicon wafer	CVD	Direct growth	[76]
WS_2	~ 0.7 nm	8-inch silicon wafer	CVD	Semi-dry	[75]
hBN	Monolayer	silicon wafer	CVD	Wet transfer	[73]
MXene	5–30 layers	silica / silicon nitride	LPE	Self-assembly	[17]
MXene	Monolayer	4-inch silicon wafer	LPE	Spin coating	[80]

B. Precise patterning

Precise device patterning is crucial for engineering the functionalities of integrated photonic devices and optimizing their performance. In industrial manufacture of bulk integrated photonic devices, the patterning of dielectric patterns (*e.g.*, waveguides) is mainly performed using photolithography, followed by etching processes such as inductively coupled plasma etching and reactive ion etching. On the other hand, the patterning of metal (*e.g.*, for electrodes and plasmonic devices) is primarily achieved through photolithography, followed by electron beam evaporation and the lift-off processes. Given that the patterning techniques for fabricating bulk integrated photonic devices has been relatively mature,[9, 81-83] here we focus on discussing the methods for patterning 2D materials in hybrid integrated devices. These include not only

conventional techniques employed for bulk integrated photonic devices, but also new methods specifically designed for 2D materials.

Photolithography is a dominant device patterning technique in the IC industry. In the photolithography process, the designed layout is transferred from a mask onto photoresist coated on an integrated substrate. Depending on the employed light wavelength, it can be categorized into ultraviolet (UV), deep ultraviolet (DUV), and extreme ultraviolet (EUV) lithography, which allow different levels of patterning resolution.[84, 85] Unlike electron-beam lithography (EBL), which achieves a higher resolution at the expense of considerably longer exposure times, photolithography is more widely employed for industrial manufacturing. In **Fig. 5(a)**, 50-nm-wide graphene nanoribbons featuring straight, clean, and parallel edges were fabricated by using a multi-patterning process that involved photolithography and bottom-up self-expansion. This method enabled a patterning resolution < 100 nm, which is one order of magnitude lower than the traditional lithographical resolution.[86] In **Fig. 5(b)**, a 50-μm-long GO film was patterned on a doped silica micro-ring resonator (MRR). The film placement and coating length were precisely controlled via photolithography on a photoresist, followed by GO film coating (through self-assembly) and lift-off processes.[87]

Nanoimprinting is another widely used patterning technique in integrated device fabrication. Compared to photolithography, it has similarities in steps like resist coating, film attachment, and resist removal, but differs by using an imprint mold to pattern the resist layer instead of photolithography. In **Fig. 5(c)**, graphene nanoring arrays were fabricated on a 9-cm^2 silica substrate via nanoimprinting. The fabricated rings had a width of <15 nm and a thickness of <0.7 nm.[88] In addition, nanoimprinting was utilized to engineer the strain of 2D MoS_2 films in **Fig. 5(d)**, allowing for precise control of the strain magnitudes and distributions at a low cost and high throughput.[89]

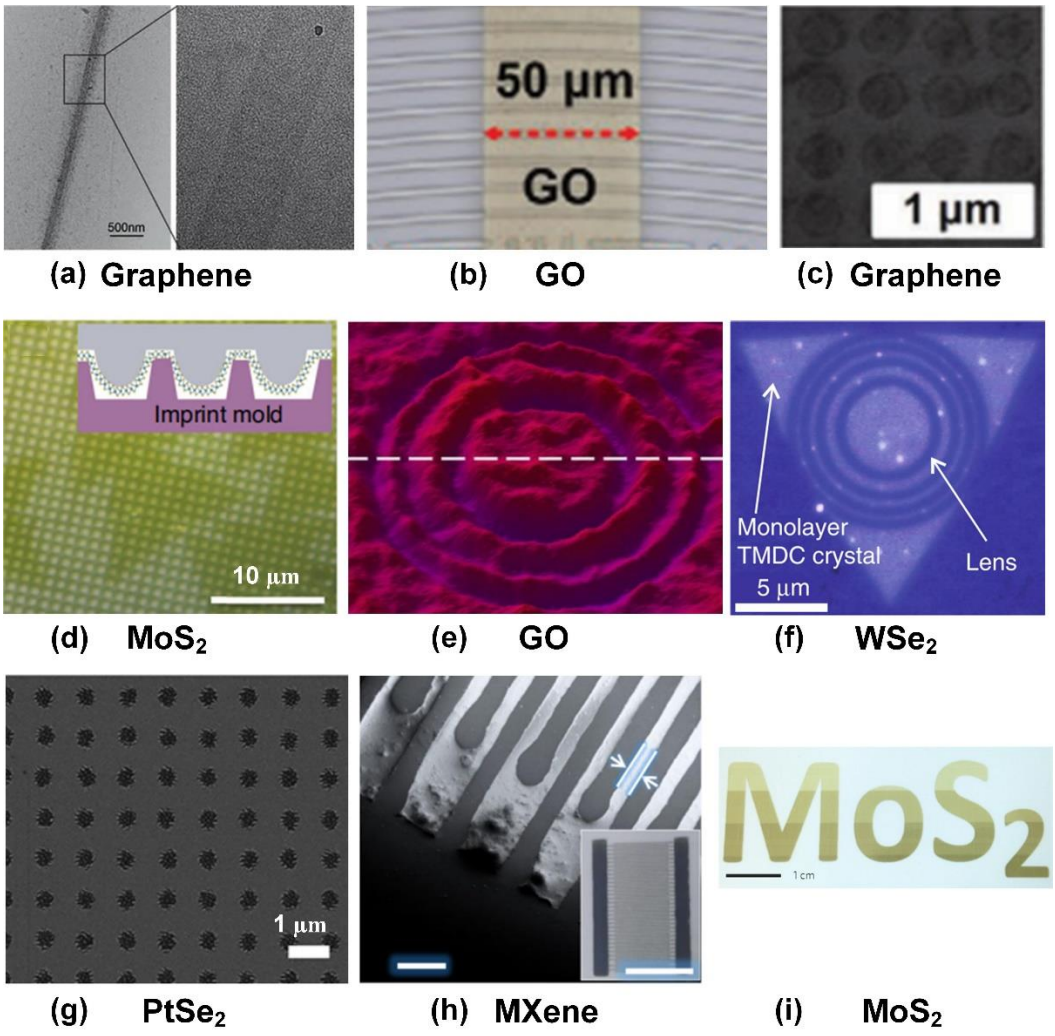

FIG. 5. Methods for patterning 2D material films on integrated substrates. (a) A graphene nanoribbon patterned via photolithography and bottom-up self-expansion. (b) A GO film patterned via photolithography and lift-off. (c) Graphene nanoring arrays patterned via nanoimprinting. (d) A MoS_2 film patterned via nanoimprinting. (e) A 200-nm-thick GO lens patterned via laser patterning. (f) A monolayer tungsten diselenide (WSe_2) lens patterned via laser patterning. (g) $PtSe_2$ nanohole arrays patterned via laser patterning. (h) MXene lines patterned via inkjet printing. (i) 'MoS_2' word printed via inkjet printing. (a) Reproduced with permission from Borhade *et al*., Small **20**(22), 2311209 (2024). Copyright 2024 John Wiley and Sons. (b) Reproduced with permission from Wu *et al*., Small **16**(16), 1906563 (2020). Copyright 2020 John Wiley and Sons. (c) Reproduced with permission from Pak *et al*., Adv. Mater. **25**(2), 199-204 (2013). Copyright 2013 John Wiley and Sons. (d) Reproduced with permission from Sun *et al*., Microsyst. Nanoeng. **10**(49) (2024). Copyright 2024 Springer Nature. (e) Reproduced with permission from Zheng *et al*., Nat. Commun. **6**, 8433 (2015). Copyright 2015 Springer Nature. (f) Reproduced with permission from Lin *et al*., Light Sci. Appl. **9**, 137 (2020). Copyright 2020 Springer Nature. (g) Reproduced with permission from Enrico *et al*., ACS Nano **17**(9), 8041-8052 (2023). Copyright 2023 American Chemical Society. (h) Reproduced with permission from Zhang *et al*., Nat. Commun. **10**(1), 1795 (2019). Copyright 2019 Springer Nature. (i) Reproduced with permission from McManus *et al*., Nat. Nanotechnol. **12**(4), 343-350 (2017). Copyright 2017 Springer Nature.

Compared to photolithography and nanoimprinting, laser patterning provides a quick and simple method for directly patterning 2D film without using any masks, molds, photoresists, or chemical solutions. In **Fig. 5(e)**, a GO flat lens was fabricated by using laser patterning to convert the GO into reduced GO (rGO) via photoreduction, achieving a focusing resolution of ~300 nm and an absolute focusing efficiency >32% over a broad wavelength range from 400 to 1500 nm.[90] In **Fig. 5(f)**, laser patterning was used for fabricating a flat lens on monolayer TMDC, achieving a subwavelength lateral resolution of ~400 nm and a high focusing efficiency of ~31%.[91] In **Fig. 5(g)**, a noncontact laser patterning method was proposed by using a two-photon 3D printer with a scanning pulsed laser. 2D materials like graphene, MoS_2, and platinum diselenide ($PtSe_2$) were patterned with a subwavelength resolution (*e.g.*, ≥100-nm hole diameter) at a high throughput (*e.g.*, ~3s to clear a 200 μm × 200 μm area).[92]

As a modified solution dropping technique, inkjet printing enables the on-chip transfer and patterning of 2D films in a single step. Its fast and in-situ patterning allows for industrial fabrication of large-area patterns, with their position and shape controlled by program. In **Fig. 5(h)**, additive-free MXene ink for was used for inkjet printing, achieving a line width of ~80 μm, a gap width of ~50 μm, and a spatial uniformity of ~3.3%.[93] In **Fig. 5(i)**, inkjet printing was used for patterning MoS_2 and graphene in large areas, with an optimal drop spacing of ~40 μm on silicon/silica substrates and ~45 μm on glass and polyethylene terephthalate.[94]

Although the aforementioned methods have been extensively used for patterning 2D materials in laboratory research and offer appealing advantages for industrial fabrication, challenges still remain. For example, photolithography has limitations induced by chemical residues after the etching or lift-off process, damage in 2D films due to high-energy exposure or aggressive chemical solutions, and reduced effectiveness on non-planar substrates. The laser patterning process can also cause damage to 2D films. In addition, the minimum feature size of laser patterning is limited by the spot size of the focused laser beam, resulting in a relatively low patterning resolution that is typically > 300 nm. Nanoimprinting face challenges related to its flexibility in changing the device pattern and in achieving a high film uniformity across

large areas. These make it better suited for fabricating relatively simple and repetitive patterns. The imprinting process can also cause mechanical damage to the delicate structures of 2D materials, thus degrading their performance for some applications. For inkjet printing, the patterning resolution is relatively low (typically > 1 μm), and it also face challenges similar to other solution dropping methods, such as low film uniformity and large film thicknesses.

Some other patterning methods, such as focused ion beam (FIB) milling,[95-97] scanning probe lithography (SPL),[98, 99] adhesion lithography,[100] and self-assembled-mask lithography (SAML),[101, 102] have also been employed for patterning 2D materials. Each method has its own distinct advantages, such as the high patterning resolution for FIB milling (*e.g.*, down to 10 nm[95]) and the rapid processing speed for SPL (*e.g.*, ~20 mm/s[103]). However, either relatively low fabrication efficiency or limited applicability to different 2D materials restrict their current use to laboratory research rather than industrial-scale production. With continued progress in micro/nano fabrication techniques, it is anticipated that more advanced patterning methods aimed at low-cost and highly efficient industrial manufacturing would be developed to overcome existing limitations in the future.

C. Dynamic tuning

Dynamic tuning underpins the operation of many active integrated photonic devices such as lasers,[10, 104] optical switches,[105, 106] and electro-optic modulators.[107, 108] Even for passive integrated photonic devices, introducing dynamic tuning is useful for optimizing their performance[87, 109] and extending their applicability across varying conditions.[110, 111] For commercial bulk integrated photonic devices, dynamic tuning is typically achieved by introducing co-integrated thermo-optic micro-heaters[112, 113] or PN junctions[114, 115] to change material refractive indices. The former has typical response times in the millisecond to microsecond range, whereas the latter enables faster tuning with response times on the order of picoseconds or even faster. In laboratory research, dynamic tuning can also be achieved through laser-induced photothermal effects or nonlinear optical effects.[116, 117] For hybrid integrated photonic devices incorporating 2D

materials, dynamic tuning of the properties of 2D materials is also crucial for enabling functionalities and optimizing performance. In this part, we discuss the mechanisms for dynamic tuning of 2D materials in hybrid integrated photonic devices, which are classified into gate tuning, laser tuning, thermal tuning, and strain tuning.

2D materials exhibiting metallic behaviors, such as graphene and TMDCs, are susceptible to external electrical fields due to their exceptional Fermi-Dirac tunability. This forms the basis of electrostatic gate tuning methods, which allows for efficient, reversible, and real-time modulation of their electrical and optical properties. In **Fig. 6(a)**, a graphene/ion-gel heterostructure was integrated on a silicon nitride MRR with source–drain and top gating, which enabled gate tuning of the Fermi level of graphene and hence the chromatic dispersion of the hybrid MRR.[118] In **Fig. 6(b)**, a monolayer WS_2 was patterned on a silicon nitride MRR with ionic liquid cladding. The WS_2 film was doped by applying a bias voltage across the two electrodes through the ionic liquid, resulting in a significant refractive index change of $\Delta n = 0.53$.[119] In **Fig. 6(c)**, ferroelectric gate tuning was achieved by co-integrating a ferroelectric P(VDF-TrFE) top layer over a 2D molybdenum diteluride ($MoTe_2$) film on a silicon/silica substrate. By using a scanning probe to control the polarization of the ferroelectric polymers, lateral p–n, n–p, p–p, n–n homojunctions were constructed in the $MoTe_2$ film, allowing simple and arbitrary definition of the carrier injection with nanoscale precision.[120]

Lasers can be used to trigger optical effects like saturable absorption, photon-excited carrier transport, and photothermal effects in 2D materials, which can, in turn, be harnessed to dynamically tune their properties. In **Fig. 6(d)**, a graphene was integrated on a silicon photonic crystal cavity, where the optical absorption of graphene was tuned via exposure to a continuous-wave (CW) laser at 1064 nm, achieving a resonance wavelength shift of ~3.5 nm and a quality factor change of ~20%.[121] In **Fig. 6(e)**, the light absorption in a graphene-silicon hybrid nanowire waveguide was tuned by exposure to a 635-nm CW laser. During the tuning process, the photon-excited carriers in silicon were injected into graphene via the Schottky diode junction, resulting in an increased carrier concentration and change of the Fermi level.[122] In **Fig. 6(f)**, by injecting a CW light into GO-silicon hybrid waveguides to induce reversible photo-

thermal changes in 2D GO films, three functionalities were demonstrated across broad wavelength ranges, including all-optical control and tuning, optical power limiting, and non-reciprocal light transmission.[123]

Apart from laser-induced photo-thermal changes, co-integrated micro-heaters can also induce photothermal changes in 2D materials. Unlike the hybrid tuning approach in **Fig. 6(f)** that combines laser and thermal tuning, the use of micro-heaters to cause temperature-dependent changes is a typical thermal tuning method. In **Fig. 6(g)**, a ring-shaped metallic microheater was fabricated on top of polypropylene, with a MoS_2 film placed at its center. By applying a bias voltage to the microheater, the temperature of the polypropylene surface was changed, enabling precise and reversible tuning of the refractive index of MoS_2.[124]

Strain tuning provides an effective method to modify the properties of 2D materials in a continuous and reversible manner by applying mechanical tension or compression. Localized strain can be utilized to finely control and adjust material properties such as optical emission and photoconductivity in 2D materials. However, in comparison to gate or optical tuning, the response time of strain tuning is relatively slow. In **Fig. 6(h)**, single photon emission in a 2D hBN film were controlled via local strain tuning induced by atomic force microscope indentation. By tuning the indentation parameters, indents sites with various lateral sizes were obtained to fully activate the single-photon emitters.[125] In **Fig. 6(i)**, single-photon emitters were achieved in a WSe_2 film by using strain tuning through nanoscale stressors combined with defect engineering via electron-beam irradiation. This method not only allowed precise tuning of the emission sites but also improved the yield, purity, and operational temperature of the emitters.[126]

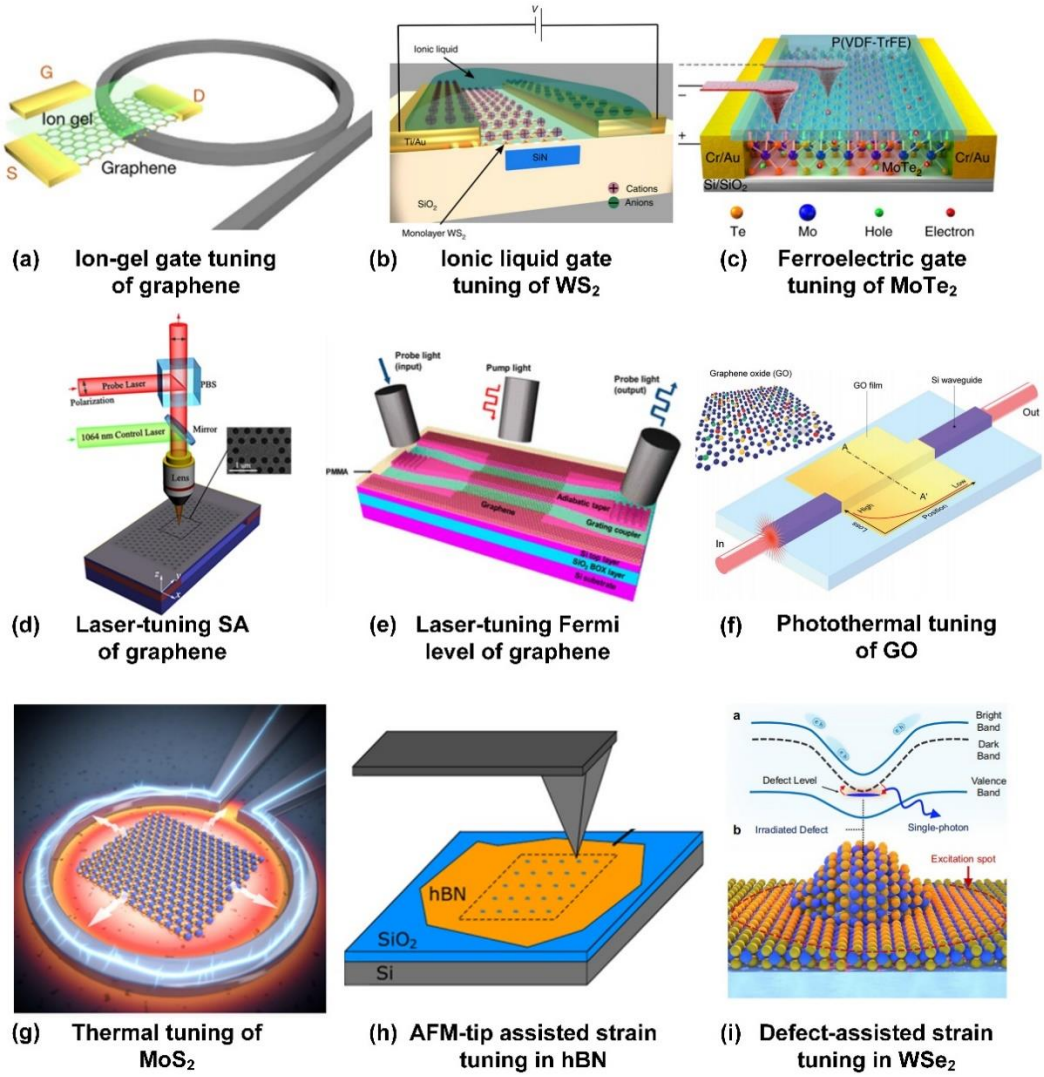

FIG. 6. Methods for dynamic tuning of 2D materials in integrated photonic devices. (a) Ion-gel gate tuning of graphene integrated on a silicon nitride MRR. (b) Ionic liquid gate tuning of WS_2 integrated on a silicon nitride MRR. (c) Ferroelectric gate tuning of $MoTe_2$ integrated on a silicon substrate. (d) Laser tuning saturable absorption (SA) of graphene integrated on a silicon photonic crystal cavity. (e) Laser tuning Fermi level of graphene integrated on silicon-on-insulator nanowires. (f) Photothermal tuning of GO integrated on a silicon waveguide. (g) Thermal tuning of MoS_2 integrated on a polypropylene substrate. (h) Atomic force microscopy (AFM)-assisted strain tuning of hBN integrated on a silicon substrate. (i) Defect-assisted strain tuning of WSe_2 integrated on a silicon substrate. (a) Reproduced with permission from Yao *et al*., Nature **558**(7710), 410-414 (2018). Copyright 2018 Springer Nature. (b) Reproduced with permission from Datta *et al*., Nat. Photonic **14**(4), 256-262 (2020). Copyright 2020 Springer Nature. (c) Reproduced with permission from Wu *et al*., Nat. Electron. **3**, 43-50 (2020). Copyright 2020 Springer Nature. (d) Reproduced with permission from Shi *et al*., ACS Photonics **2**(11), 1513-1518 (2015). Copyright 2015 American Chemical Society. (e) Reproduced with permission from Yu *et al*., ACS Photonics **8**(11), 11386−11393 (2014). Copyright 2014 American Chemical Society. (f) Reproduced with permission from Wu *et al*., Adv. Mater. **36**(16), 2403659 (2024). Copyright 2024 John Wiley and Sons. (g) Reproduced with permission from Ryu *et al*., Nano Lett. **20**(7), 5339-5345 (2020). Copyright 2020

American Chemical Society. (h) Reproduced with permission from Xu *et al*., Nano Lett. **21**(19), 8182-8189 (2021). Copyright 2021 American Chemical Society. (i) Reproduced with permission from Parto *et al*., Nat. Commun. **12**(1), 3585 (2021). Copyright 2021 Springer Nature.

Although the above dynamic tuning methods of 2D materials offer attractive benefits, several challenges still need to be addressed for their use in industrial fabrication. For instance, traditional gating tuning methods often struggle to achieve precise modulation in small, localized regions. This lack of precision can limit the effectiveness of tuning, especially for nanoscale devices. For laser tuning method, the tuning lasers are usually not co-integrated on chips, which hinders its wide use for commercial products. In addition, improper laser intensity or wavelength can result in localized overheating or photodegradation of 2D materials, leading to irreversible damage such as ablation or defect formation. Some strain tuning methods are prone to damage the 2D materials during the tuning process such as cracking, folding, or tearing, especially when the strain exceeds the material elastic limit. The relatively low response speed of strain tuning also limits its use in high-speed tuning applications. To address these challenges, it is expected that future advancements in dynamic tuning methods would be developed with more robust, flexible, and versatile control.

D. Packaging

Device packaging typically represents the final stage of integrated device fabrication, where the device is encapsulated in a protective case that safeguards it from physical damage and corrosion. This step is essential for the industrial manufacturing of commercial products with stable operation. After over 50 years of development, the IC industry has already established well-developed packaging techniques, such as pin grid array (PGA), land grid array (LGA), ball grid array (BGA) and 2D & 3D customized solutions.[127-130] With respect to PICs, some advanced packaging techniques have been adapted from those used for ICs, while also taking into account new factors such as fiber-to-chip coupling, chip-to-chip coupling, high-density electrical and optical interconnections, hybrid integration of photonic chips, multi-chip modules, and thermal management. **Figs. 7(a) – (c)** show some images that showcase state-of-the-art

packaging techniques for integrated photonic devices. **Fig. 7(a)** shows a hybrid tunable laser butterfly packaged by the LioniX International corporation, which includes active gain medium and a passive external cavity.[131] **Fig. 7(b)** shows a packaging technique developed by PHIX corporation, which utilizes off-the-shelf building blocks and provides an open architecture that accommodates devices with various sizes and across different integrated platforms.[132] **Fig. 7(c)** shows the first-ever fully integrated optical compute interconnect chiplet co-packaged with a Central Processing Unit (CPU) from the Intel corporation.[133]

For hybrid integrated photonics devices incorporating 2D materials, in addition to packaging integrated chips, encapsulating 2D materials is also necessary to prevent material degradation and ensure stable operation. Due to their large surface area and ultralow film thicknesses, many 2D materials (*e.g.*, BP and TMDCs) are highly sensitive to environmental factors such as temperature, humidity, mechanical stress, and chemical exposure. To improve their stability in hybrid integrated devices, various encapsulation materials, such as dielectric materials, organic polymers, and robust 2D materials, have been used to effectively shield 2D materials from the surrounding environment.

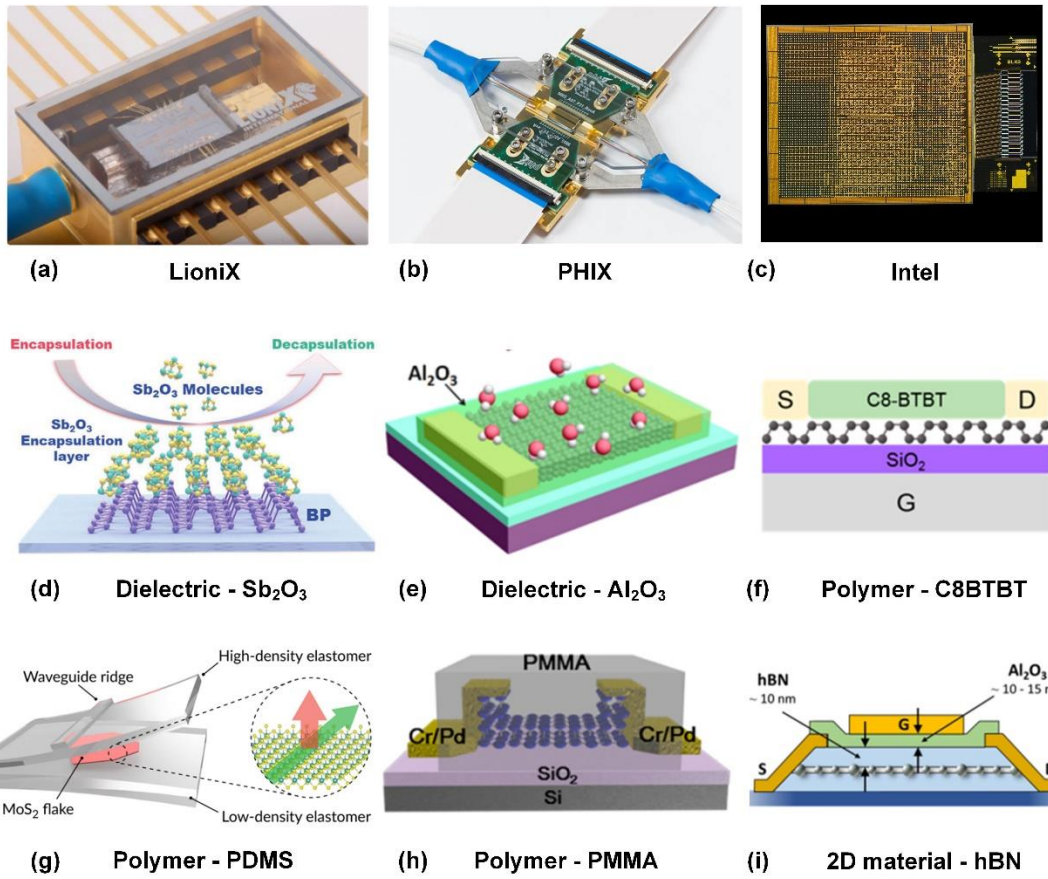

FIG. 7. Methods for packaging PICs and encapsulation of 2D materials in hybrid integrated photonic devices. (a) A hybrid tunable laser packaged by the LioniX International corporation. (b) A packaging module for photonic devices with an open architecture from PHIX corporation. (c) An integrated optical compute interconnect chiplet packaged by the Intel corporation. (d) Encapsulation of a BP film by covering a 3-nm-thick inorganic molecular crystal Sb_2O_3 layer. (e) Encapsulation of a BP film by covering a 6-nm-thick Al_2O_3 layer. (f) Encapsulation of a BP film by covering a 60-nm-thick C8-BTBT organic film. (g) Encapsulation of a MoS_2 film in a polydimethylsiloxane (PDMS) waveguide chip. (h) Encapsulation of a BP film by covering a 300-nm-thick polymethyl methacrylate (PMMA) polymer layer. (i) Encapsulation of a graphene film between two hBN layers. (a) Reproduced from https://www.lionix-international.com/photonics/pic-technology/assembly-and-packaging-service/. (b) Reproduced from https://www.phix.com/our-offering/prototype-package/phix-characterization-package/. (c) Reproduced from https://www.intel.com/content/www/us/en/newsroom/news/intel-unveils-first-integrated-optical-io-chiplet.html#gs.gpexcr. (d) Reproduced with permission from Liu *et al.*, Adv. Mater. **34**(7), e2106041 (2022). Copyright 2022 John Wiley and Sons. (e) Reproduced with permission from Miao *et al.*, ACS Appl. Mater. Interfaces **9**(11), 10019-10026 (2017). Copyright 2017 John Wiley and Sons. American Chemical Society. (f) Reproduced with permission from He *et al.*, Nano Lett. **19**(1), 331-337 (2019). Copyright 2019 American Chemical Society. (g) Reproduced with permission from Auksztol *et al.*, ACS Photonics **6**(3), 595-599 (2019). Copyright 2019 American Chemical Society. (h) Reproduced with permission from Jia *et al.*, ACS Nano **9**(9), 8729-8736 (2015). Copyright 2015 American Chemical Society. (i) Reproduced with permission from Viti *et al.*, Nano Lett. **20**(5), 3169-3177 (2020). Copyright 2020 American Chemical Society.

In **Fig. 7(d)**, by using 3-nm-thick inorganic molecular crystal Sb_2O_3 as a protective layer, BP exhibited significantly enhanced structural stability for over 80 days, in contrast to the rapid degradation of unprotected BP within hours.[134] In **Fig. 7(e)**, a 6-nm-thick Al_2O_3 encapsulation layer was deposited on a BP film via atomic layer deposition, enabling the realization of air-stable BP-based humidity /chemical sensors.[135] In **Fig. 7(f)**, the stability of BP was improved by using a 60-nm-thick dioctylbenzothienobenzothiophene (C8-BTBT) organic film, which provided protection against oxidation under ambient conditions for more than 20 days. This approach can also be applied to other 2D materials such as TMDCs.[136] In **Fig. 7(g)**, a monolayer of MoS_2 was embedded within an elastomeric waveguide chip made from polydimethylsiloxane (PDMS), which not only ensured mechanical and environmental protection of the MoS_2 film but also enhanced its photoluminescence (PL) performance.[137] In **Fig. 7(h)**, BP films were plasma-treated and passivated with a ~300-nm-thick PMMA polymer cover layer, which not only eliminated chemical degradation of the oxidized BP surface but also provided protection against water and oxygen molecules in the air.[138] In **Fig. 7(i)**, a monolayer graphene film was encapsulated between two hBN layers (~30 nm on the bottom and ~10 nm on the top) with high thermal, chemical, and mechanical stability, allowing for broadband and low-noise terahertz photodetection at room temperature.[139]

Although the above encapsulation methods provide many advantages in protecting 2D materials from environmental degradation, they still present some limitations in terms of broad applicability and long-term performance needed for commercial products. For instance, physical encapsulation with polymers like PMMA suffers from limited durability and will degrade rapidly when exposed to organic solvents. In addition, the encapsulation with dielectric materials such as Al_2O_3 via atomic layer deposition method and chemical functionalization with organic solutions is destructive, leading to inevitable degradation of the properties of 2D materials. The encapsulation methods such as dielectrics deposition and polymer coatings may also compromise the sensitivity and functionality of 2D materials in integrated photonic devices, resulting in a trade-off between protection and performance. Therefore, it is expected that more

non-invasive encapsulation methods would be developed in the future, not only providing enhanced protection for 2D materials against environmental degradation, but also allowing their potential to be fully exploited.

IV. COMMERCIALIZATION ISSUES

To ensure efficient manufacturing of reliable commercial products, it's necessary to consider several factors beyond fabrication techniques. In this section, we discuss some issues related to commercialization of integrated photonic devices incorporating 2D materials. It is divided into four parts, including fabrication standards, product recycling, service life, and environmental implications.

A. Fabrication standards

In industrial manufacturing, establishing clear and detailed fabrication standards is crucial for ensuring product consistency and reproducibility. For bulk integrated photonic devices, comprehensive fabrication standards have already been established, such as IEC Technical Report 63072 by the International Electrotechnical Commission (IEC)[140] and ISO-10110 by the International Organization for Standardization (ISO).[141] However, for integrated photonic devices incorporating 2D materials, there is still a lack of unified protocols or fabrication standards in the manufacturing processes.

Since the properties of 2D materials are affected by the fabrication methods, the quality and consistency of synthesized materials in practical settings vary widely, which has limited its large-scale industrial applications. To enable accurate evaluations and comparisons of the quality of 2D materials, it is essential to establish widely recognized and quantitative certification standards. In this part, we discuss the possibility of establishing fabrication standards for evaluating the quality of 2D materials in hybrid integrated devices. These standards can guide the selection and characterization of 2D materials for industrial manufacturing, ensuring that they meet specific performance criteria necessary for commercial products.

TABLE II. Typical characterization methods for assessing quality and properties of 2D materials. XPS: X-ray photoelectron spectroscopy; XRD:X-ray diffraction; UV-VIS: ultraviolet-visible; AFM: atomic force microscopy; SEM: scanning electron microscopy; TEM: transmission electron microscopy; HRTEM: high-resolution transmission electron microscopy; STEM: scanning transmission electron microscopy; PL: photoluminescence.

Methods	Main features	Ref.
Raman spectroscopy	Analyzing chemical composition, molecular vibrations, crystal structure, and defect density by measuring the shift in laser photon energy caused by Raman scattering during light-matter interaction	142
XPS	Analyzing elemental composition and chemical states by measuring the energy of photoelectrons emitted from the surface after X-ray irradiation	143
XRD	Analyzing crystal structure and phase by measuring the angles of X-ray diffraction and the intensities of the resulting diffraction peaks	144
UV-VIS spectrometry	Measure the absorption of ultraviolet and visible light passing through a sample to identify and quantify various compounds	145
AFM	Topographic imaging to characterize film thickness / uniformity, and force measurement to characterize sample mechanical properties	146
Optical microscopy	Imaging sample surface by using a system of optical lenses, the maximum magnification typically ranges from 500X to 1500X	147
SEM	Imaging sample surface by scanning a focused electron beam, the maximum magnification typically ranges from 10,000X to 500,000X	148
TEM	Imaging internal structure at atomic level by transmitting a beam of high-energy electrons through thin samples, the maximum magnification typically ranges from 100,000X to 1,000,000X	149
HRTEM	A high-resolution imaging mode of specialized TEM that allows for direct imaging of the atomic structure of samples	150
STEM	Combining SEM and TEM for high-resolution atomic-scale imaging	151
PL	Measuring light emission from materials under optical excitation to analyze optical properties of samples	152
Carrier mobility	Measuring mobility of charge carriers when subjected to external electric fields to characterize electrical properties of samples	153

Table II provides an overview of typical methods for characterizing the quality and properties of 2D materials. In laboratory research, Raman spectroscopy is the most widely used approach for characterizing the properties of 2D materials. By measuring

the shift in laser photon energy induced by Raman scattering, it can be used to analyze the molecular vibrations, crystal structure, chemical composition, and defect density in samples. For example, the intensity ratios of *D* to *G* peaks (I_D/I_G) obtained from the Raman spectra are useful for characterizing the properties of graphene family materials. In **Fig. 8(a)**, the change of I_D/I_G in the measured Raman spectra indicates different levels of reduction in a GO film after applying different input light powers.[154] In addition, the quality of TMDCs can be assessed by analyzing the variations of E_{2g} and A_{1g} peaks in Raman spectra. In **Fig. 8(b)**, after oxygen plasma exposure treatment on pristine monolayer MoS_2, the intensities of both E_{2g} and A_{1g} peaks show a significant decrease, indicating a substantial increase in lattice distortion in the MoS_2 crystal.[155]

In addition to Raman spectroscopy, X-ray photoelectron spectroscopy (XPS), X-ray diffraction (XRD), and ultraviolet-visible (UV-VIS) spectrometry are also useful methods for characterizing the properties of 2D materials. XPS is a quantitative spectroscopic method that generates electron population spectra by irradiating a material with a beam of X-rays. It can be used to characterize the elemental composition of a material and its chemical state. **Fig. 8(c)** shows an XPS spectra for MoS_2 films synthesized by a modified tetraheptylammonium bromide (THAB)-exfoliated method compared with a traditional lithium (Li)-exfoliated method.[66] Analyzing the *3d* peaks for Mo and *2s* peak for S reveals that the modified method yields a pure 2H phase of MoS_2, whereas the Li-exfoliated MoS_2 nanosheets are predominantly in the 1T phase. XRD is widely used to characterize crystal structure and phase by measuring the angles of X-ray diffraction and the intensities of the resulting diffraction peaks. **Fig. 8(d)** shows a real-time peak shift to a higher angle in the XRD spectra for a $Ti_3C_2T_x$ MXene film, indicating a decreased interlayer spacing due to the removal of water and adsorbents after N_2 purging.[156] UV-VIS spectrometry measures the absorption spectra of a sample as ultraviolet and visible light passes through it. This technique is widely employed to identify and quantify various compounds in a variety of samples. Compared to XPS, UV-VIS can analyze the properties of samples in both film and solution forms. **Fig. 8(e)** shows UV-VIS spectra to qualitatively analyze the percentage of few-layer GO sheets in dispersions by

comparing the absorption peak intensities.[157]

Although the above material characterization methods provide useful tools for quantitatively analyze the atomic structure and chemical characteristics of 2D materials, they have limitations in accurately assessing physical characteristics such as film thickness, surface uniformity and adhesion between 2D materials and integrated substrates. To characterize the film thickness and uniformity, atomic force microscopy (AFM) can be employed. **Fig. 8(f)** shows an AFM image of a monolayer GO film fabricated by the solution-based self-assembly method, which had a thickness of ~1 nm and a high uniformity.[67] In addition, some other microscopy methods, such as optical microscopy, scanning electron microscopy (SEM), transmission electron microscopy (TEM), high-resolution transmission electron microscopy (HRTEM), scanning transmission electron microscopy (STEM), and scanning tunneling microscopy (STM), can be used to examine surface morphology, wrinkles, and interface characteristics between different materials. **Fig. 8(g)** shows an SEM image of an SOI nanowire waveguide coated with monolayer of GO, confirming the conformal coating of the 2D films onto the waveguide.[70] **Fig. 8(h)** shows a cross-sectional STEM image of the interface between stacked Au electrodes and 1T'-ReS_2 films, clearly indicating a gap of ~3.7 Å at the interface.[158]

Another widely used approach to assessing the quality of 2D materials is to characterize their optical or electrical properties. For instance, the measured PL spectra in **Fig. 8(i)** show a significant quenching in the overlapping area between MoS_2 and WS_2, which indicates strong interaction between the two materials and the clean interface of the 2D heterostack.[74] In **Fig. 8(j)**, the carrier mobilities of graphene was measured after transferring onto silicon substrates via a modified wet transfer method, ranging between 70,000 and 120,000 $cm^2\ V^{-1}\ s^{-1}$ at room temperature. These values surpass the standard value of ~30,000 $cm^2\ V^{-1}\ s^{-1}$ for conventional wet transfer methods, reflecting the high-quality of graphene transferred by this new method.[72]

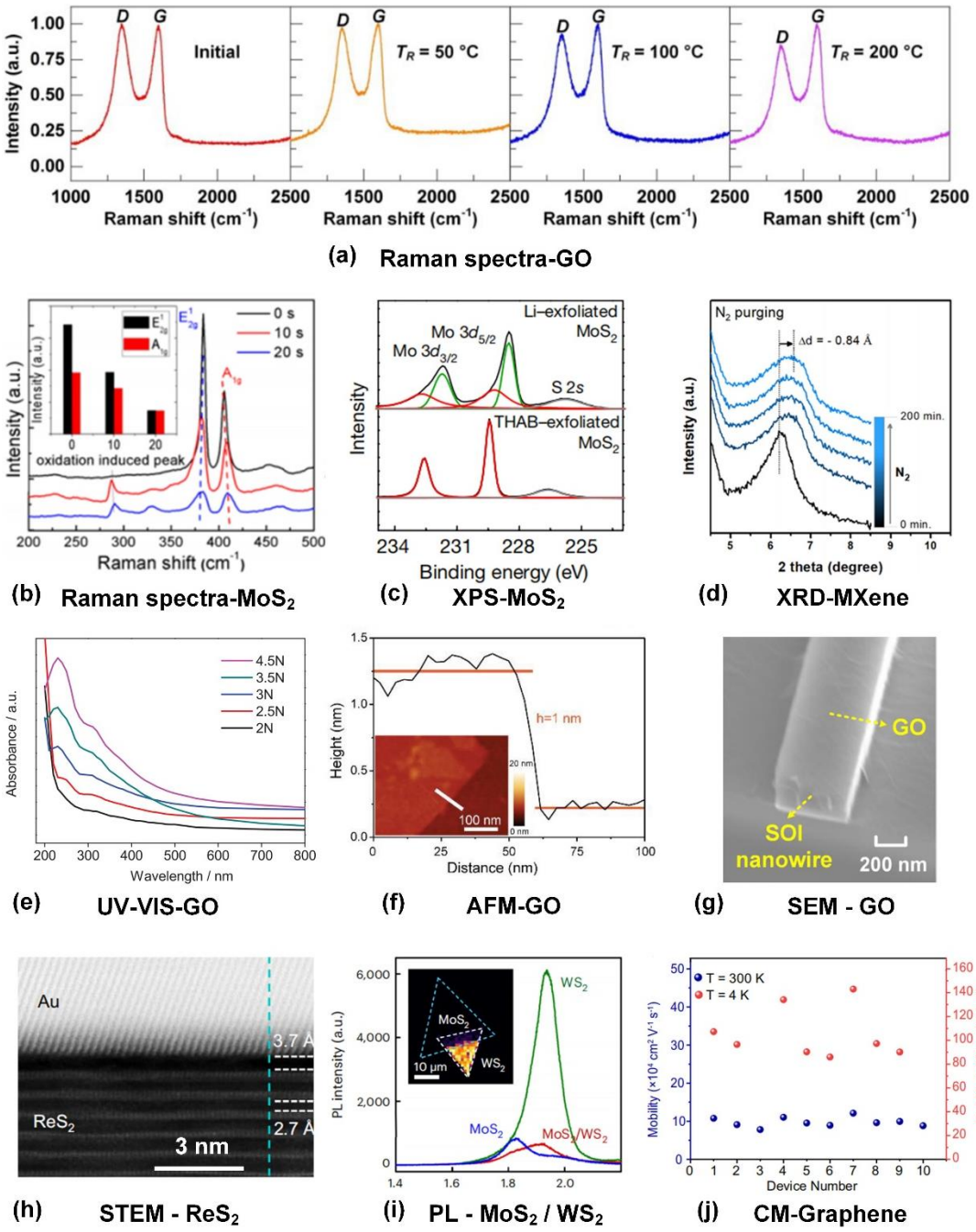

FIG. 8. Methods for evaluating quality of 2D materials. (a) Raman spectra of GO at different levels of reduction. (b) Raman spectra of MoS_2 before and after oxygen plasma exposure treatment. (c) X-ray photoelectron spectra (XPS) of MoS_2 synthesized by two different liquid-phase exfoliation methods. (d) X-ray diffraction (XRD) spectra of $Ti_3C_2T_x$ MXene film after N_2 purging. (e) Ultraviolet-visible (UV-VIS) spectra of GO dispersions. (f) Atomic force microscopy (AFM) image of a monolayer GO film. (g) Scanning electron microscopy (SEM) image of monolayer GO conformally coated on a silicon waveguide. (h) Scanning transmission electron microscopy (STEM) image of the interface between stacked Au electrodes and 1T'-ReS_2 films. (i) Photoluminescence (PL) spectra in the overlapping area between MoS_2 and WS_2. (j) Carrier mobilities (CM) of graphene after being transferred onto silicon substrates. (a) Reproduced with permission from Hu *et al.*, Adv. Funct. Mater. 2406799 (2024). Copyright

2024 John Wiley and Sons. (b) Reproduced with permission from Ye *et al*., Nano Lett. **16**(2), 1097-103 (2016). Copyright 2016 American Chemical Society. (c) Reproduced with permission from Lin *et al*., Nature **562**(7726), 254-258 (2018). Copyright 2018 Springer Nature. (d) Reproduced with permission from Lai *et al*., AIP Advances **2**(3), 032146 (2012). Copyright 2012 AIP Publishing. (e) Reproduced with permission from Yang *et al*., ACS Photonics **6**(4), 1033-1040 (2019). Copyright 2019 American Chemical Society. (f) Reproduced with permission from Zhang *et al*., ACS Appl. Mater. Interfaces **12**(29), 33094-33103 (2020). Copyright 2020 American Chemical Society. (g) Reproduced with permission from Zhang *et al*., Nat. Commun. **15**(1), 4619 (2024). Copyright 2024 Springer Nature. (h) Reproduced with permission from Nakatani *et al*., Nat. Electron. **7**, 119-130 (2024). Copyright 2024 Springer Nature. (i) Reproduced with permission from Zhao *et al*., Nat. Commun. **13**(1), 4409 (2022). Copyright 2022 Springer Nature.

Now the aforementioned methods are mainly used for laboratory research and need to address some limitations before they can be applied more widely in industrial production. For instance, Raman spectroscopy requires high film uniformity when characterizing ultrathin (< 10 nm) 2D films. Increased film roughness can lead to higher scattering loss, which in turn impacts the accuracy of the measurements. In addition, although some advanced instruments like TEM, HRTEM, STEM, and STM can offer exceptional accuracy in characterizing 2D materials, they often come with high costs for acquisition, operation, and maintenance, potentially limiting their widespread adoption in industrial environments. Testing optical and electrical properties of 2D films involve more complex procedures and specialized instruments. It is also sensitive to temperature fluctuations, which can lead to inconsistent results in varying conditions. Characterizing each individual device can be a time-consuming process. Therefore, extensive sampling and statistical analysis are required during large-scale production to guarantee consistent material quality across various batches. In the future, it is expected that some more general and cost-effective methods such as Raman spectroscopy and AFM will initially be employed in industrial production, and these methods will gradually evolve into automatic and high-throughput characterization processes with high consistency, high efficiency, and low cost.

B. Recycling

In the early history of ICs, damaged integrated devices were deemed unsuitable for reuse and were usually discarded. However, with the rapid advancement of

fabrication techniques, modern recycling technologies have changed the way for handling discarded integrated devices. The recycling of these devices provides a sustainable alternative to their disposal with added benefits such as resource conservation, cost reduction, environmental impact reduction, and circular economy promotion. For bulk integrated photonic devices, the recycling process typically involves chemical etching, mechanical polishing, and hydrothermal treatments,[159-161] ensuring that the recycled devices meet the necessary standards for reuse in new fabrication. In hybrid integrated photonic devices incorporating 2D materials, the ultrathin 2D films tend to be more susceptible to damage compared to the bulk integrated devices. In most cases, damage is only limited to 2D materials themselves. Therefore, the removal and retransfer of 2D films are crucial for reusing these devices, particularly given that fabricating new integrated devices is usually more intricate and costly than recoating 2D films.

Fig. 9 illustrates typical processes for recycling hybrid integrated photonic devices incorporating 2D materials. First, 2D materials are transferred and patterned on bare integrated photonic devices to fabricate a product for use. Next, the fabricated device experiences damage to the 2D materials due to factors such as exposure to high temperature, humid environment, bending or stretching, and exposure to high-power laser irradiation. Finally, the undamaged integrated photonic device is reused for a new product after removing the damaged 2D film and recoating a new one, which also represents the start of a new cycle.

Flat polymer films, such as PDMS or PMMA, have been employed for mechanically peeling off 2D materials from underlying substrates.[162] This technique leverages strong adhesion between the polymer and the 2D material, allowing for effective removal of 2D materials without introducing chemical contaminants and significant damage to the substrates. In addition, wet-chemical etching, which typically employes specific solvents like acetone, acid, and tetramethylammonium hydroxide, facilitates selective dissolution of certain 2D materials such as GO and TMDCs.[163] It allows for controlled removal of 2D films while preserving the integrity of neighboring structures. Oxygen plasma treatment via reactive ion bombardment can efficiently

oxidize and etch away 2D films like GO, TMDCs and BP, and maintain minimal impact on the remaining components.[164] Laser ablation employs focused laser pulses to vaporize or break chemical bonds in target areas, offering a highly localized and non-contact method for the precise removal of 2D films with minimal thermal damages. It has been used to effectively remove graphene and hBN.[165]

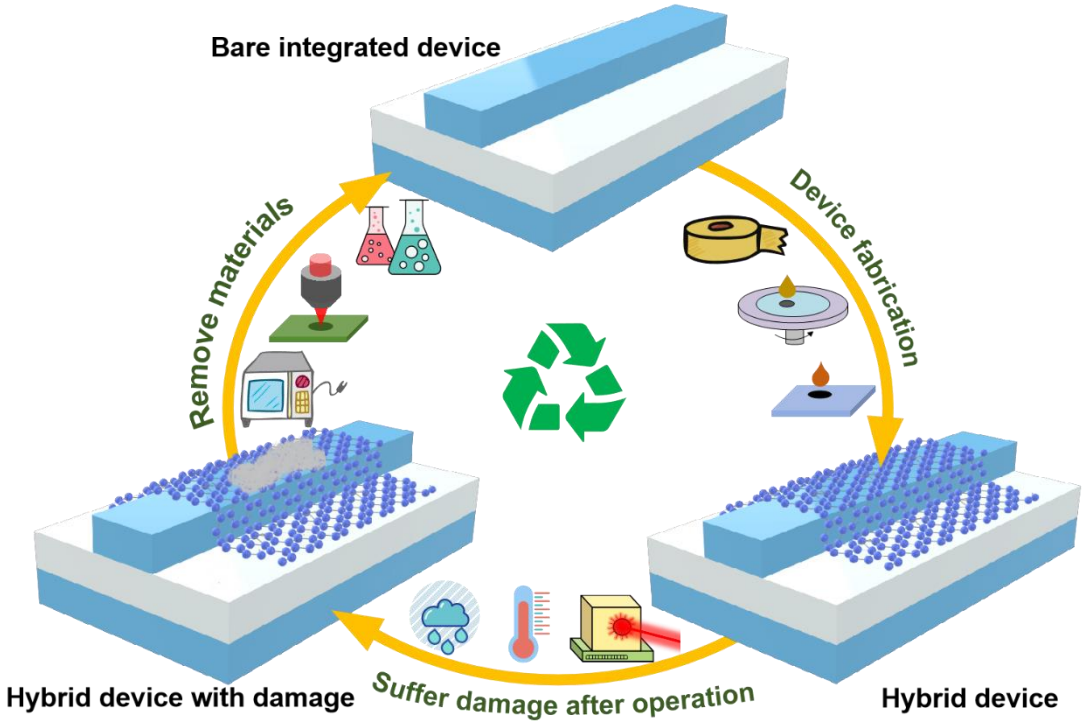

FIG. 9. Recycling of hybrid integrated photonic devices incorporating 2D materials.

To date, the recycling techniques mentioned above are mainly used in laboratory research, and there are several challenges associated with their implementation in sustainable industrial manufacturing processes. First, the aforementioned recycling methods are more widely employed for passive integrated photonic devices. For active integrated photonic devices such modulators, switches, and photodetectors, electrodes are typically placed on top of the 2D films. Consequently, recycling these devices involves more complex processes and incurs higher costs. In addition, the recycling costs should be weighed against production costs. Integrated devices are typically produced on a wafer scale, featuring multiple devices on a single wafer. Recoating a single compact device with 2D materials may involve more complex processes and operations compared to doing so on an entire wafer, particularly given that additional

alignment tools are needed to ensure the precise placement of 2D films on the target integrated photonic devices. As a result, the recycling process can be more costly than producing a new device from a batch at the wafer scale. Driven by ongoing advancements in technology and growing awareness of sustainability, more devices recycling techniques are expected to develop such as modular designs and flexible disassembly,[166] leading to further reduced recycling costs.

C. Service life

The service life is a crucial indicator of the quality of commercial products. In industrial production, improving fabrication technology to extend service life is critical for boosting product competitiveness and appeal. Conventional IC devices have different lifespans depending on their ambient conditions and using frequency, which typically range from 3 to 10 years.[167] Given the fact that 2D materials are typically more sensitive to environmental factors than bulk integrated devices, the service life of hybrid integrated devices incorporating 2D materials can be shortened.

To improve the service life of hybrid integrated devices, it is necessary to understand the degradation mechanisms of 2D materials and make targeted improvements. One of the dominant mechanisms is the presence of water and oxygen in the air. Taking BP as an example, BP flakes are highly hydrophilic, and long-term exposure to air leads to etching of the material.[168, 169] Testing results showed that degradation begins to occur on BP surface after about one hour of exposure to air.[170] In addition, theoretical calculations show that dipole-dipole interactions between water molecules and phosphorene can induce substantial lattice distortion, shrinking the lattice by ~25% and altering the band gap by ~20%.[169] Experimental demonstrations also show that few-layer BP flakes immersed in oxygen-enriched water were completely etched away,[171] reflecting the rapid degradation of BP caused by the combined effects of oxygen and water. Aside from BP, even highly stable 2D materials like graphene can experience performance degradation caused by water and oxygen, particularly for highly sensitive devices such as modulators and photodetectors.[29, 57, 172, 173]

Another important mechanism is light-induced oxidation, where incident light serves as an excitation source to trigger chemical reactions between the materials and oxygen. This process could generate reactive oxygen species that interact with 2D materials such as BP and TMDCs, resulting in structural alterations, loss of crystallinity, and diminished electronic or optical properties. Studies have shown that UV light is the main catalyst for this oxidation process, with the degree of oxidation increasing in proportion to the light intensity. Due to the quantum confinement effect, the degree of degradation is also influenced by the thicknesses of 2D films.[169]

The degradation mechanisms mentioned above can be enhanced by increasing temperatures, which accelerate chemical reactions that undermine material integrity and result in increased degradation rates. Studies have shown that rising temperatures can increase defect mobility and exacerbate thermal effects on the electrical and optical properties of many 2D materials. For instance, high temperatures in MoS_2 can cause sulfur vacancies that disrupt the crystal structure and alter the bandgap.[174] In addition, increasing temperatures in GO can break the chemical bonds between the oxygen-containing functional groups and the carbon network, resulting in the reduction of GO and changes in its properties.[123]

Some other degradation mechanisms can also affect the stability and performance of 2D materials in hybrid integrated devices. Mechanical stress, for instance, can introduce defects in the crystal lattice, leading to a decrease in electrical conductivity and optical performance. The stress can arise from external forces or thermal expansion mismatches between 2D films and their substrates, which could result in cracking or delamination. In addition, 2D films can easily adsorb dust and other airborne contaminants, which, when combined with other mechanisms such as temperature fluctuations and mechanical stress, create synergistic effects that further accelerate their degradation.

To avoid the degradation arising from the above factors, various encapsulation methods have been investigated, as we discussed in **Part D** of **Section III**. In recent years, growing attention has focused on extending the service life of integrated photonic devices incorporating 2D materials. For example, a graphene-BP photodetector with

long-term stability was demonstrated in Ref. [175], where the robust graphene functioned as both an encapsulation layer and a highly efficient transport layer. Under ambient conditions, the device's photoresponsivity exhibited a minimal change of ~6% after 60 days of operation under consistent illumination. This represents a significant improvement in the service life compared to a pure BP device under similar conditions. In Ref. [176], $CsPbI_3$ perovskite solar cells with high stability were demonstrated, where a 2D $Cs_2PbI_2Cl_2$ capping layer was deposited between the perovskite active layer and the hole-transport layer. These devices did not degrade at 35°C and degraded by 20% of their initial efficiency for over 2100 hours at 110°C under constant illumination, significantly outperforming the degradation of 80% within few hundred to thousand hours reported for other perovskite solar cells. When operating continuously at 35°C, it is predicted that the lifetime of the encapsulated solar cells can reach 51,000 ± 7000 hours (*i.e.*, >5 years).

Besides improvements in device fabrication, it is crucial to regulate environmental conditions during storage and use to maximize the service life of related products. For instance, maintaining low humidity levels can help prevent degradation caused by moisture, and temperature control can minimize thermal effects and related damage. Furthermore, shielding devices from direct light exposure, especially UV light, can lower the risk of light-induced degradation, thereby extending the service life of hybrid integrated devices.

D. Environmental implications

Another important issue to consider when developing commercial products is their environmental implications. From the start of production through to end-of-life disposal, commercial products have many potential environmental implications that can possibly cause air, soil, and water pollution, as well as potential health risks such as released toxic gases and remnant toxic waste.

For bulk integrated photonic devices, the CMOS fabrication processes can involve environmental implications. For example, photoresist and developing solution used for photolithography typically have high toxicity and corrosiveness, and improper handling

or disposal of these chemicals can lead to contamination of soil and water.[177] In addition, the CMOS production lines are featured by high electrical energy consumption, and this energy-intensive nature leads to increased carbon emission that will exacerbate climate change.[178, 179] Greenhouse gases, such as fluorinated compounds (*e.g.*, SF_6, NF_3, CF_4, CHF_3), are commonly used for dry etching, cleaning CVD chambers, and epitaxial material growth, which also have a negative environmental impact.[179] Along with the rapid progress in commercialization of related products and development of fabrication techniques, many environmental issues for the IC industry have been adequately considered and effectively mitigated in modern manufacturing facilities, steering the entire industry toward enhanced sustainability.

Compared with bulk integrated photonic devices, on-chip integration of 2D materials involves additional fabrication processes that may present new environmental challenges. For instance, the synthesis of TMDCs such as MoS_2 often involves toxic precursors like hydrogen sulfide (H_2S) or selenium (Se), which can pose health risks and environmental hazards.[180] The wet-transfer method involves various solvents and chemicals, such as isopropanol and acid, which are harmful if directly released into the environment.[72] The reaction process in CVD can produce waste gases that may contain unreacted precursors such as metalorganic compounds, silanes, as well as toxic byproducts like hydrogen chloride and volatile organic compounds, which can also contaminate air and water.[181] The device packaging often involves some non-biodegradable materials such as PMMA and PDMS, which may lead to waste disposal issues.[137, 138]

In addition to environmental pollution generated during the fabrication process, 2D materials themselves can exhibit toxicity and pose health risks to humans. Small 2D material flakes can easily be transported and accumulated in cells or respiratory tract after inhalation.[182] Studies have shown that the in vivo toxicity of 2D materials is significantly influenced by the preparation methods, along with factors such as flake size, surface area, thickness, and the amount and type of oxygen functionalization groups. It was also found that the toxicity of TMDCs was lower than of GO, and BP exhibited toxicity levels that were intermediate between GO and TMDCs.[183] This work

will benefit all microcomb based applications[184 – 207], particularly microwave photonics [208 – 242], as well as potentially being able to exploit novel 2D nonlinear materials [243 – 273] and structures[274 – 352].

To date, research on the environmental implications of hybrid integrated devices incorporating 2D materials remains relatively limited. With continuous advancements in fabrication techniques and commercialization, it is expected that increasing focus will be placed on the environmental implications of relevant products. In the future, more environment-friendly materials and fabrication methods will be adopted to replace those that are prone to generating toxic byproducts. The shift towards sustainable solutions will not only benefit the environment but also align with consumer demands for greener products, which will ultimately foster a more responsible and sustainable industry for developing relevant products.

V. CONCLUSION

Facilitated by the superior properties of 2D materials and the rapid progress in related fabrication techniques, hybrid integrated photonic devices incorporating these promising materials are rapidly advancing towards industrial manufacturing and commercialization. In this paper, we provide a perspective on the developments of this field. We first provide an overview of recent progress towards commercialization. Next, we summarize state-of-the-art fabrication techniques, and highlight both their advantages and limitations in relation to industrial manufacturing. Finally, we address key considerations for commercialization, including fabrication standards, recycling, service life, and environmental implications. In the future, we believe that the enhanced collaboration between academia and industry will further liberate research on 2D material integrated photonics from lab, leading to more and more reliable commercial products that are easily accessible to end users.

Conflict of Interest

The authors have no conflicts to disclose.

REFERENCES

1. J. S. C. Kilby, “Turning potential into realities: The invention of the integrated circuit (Nobel lecture),”ChemPhysChem **2** (8-9), 482-489 (2001).
2. Z. Zheng, L. Zhang, W. Song, S. Feng, H. Xu, J. Sun, S. Yang, T. Chen, J. Wei and K. J. Chen, “Gallium nitride-based complementary logic integrated circuits,”Nat. Electron. **4** (8), 595-603 (2021).
3. P. R. Gray, P. J. Hurst, S. H. Lewis and R. G. Meyer, *Analysis and design of analog integrated circuits*. (John Wiley & Sons, 2024).
4. W. Bogaerts, D. Pérez, J. Capmany, D. A. Miller, J. Poon, D. Englund, F. Morichetti and A. Melloni, “Programmable photonic circuits,”Nature **586** (7828), 207-216 (2020).
5. Y. Liu, Z. Qiu, X. Ji, A. Lukashchuk, J. He, J. Riemensberger, M. Hafermann, R. N. Wang, J. Liu and C. Ronning, “A photonic integrated circuit–based erbium-doped amplifier,”Science **376** (6599), 1309-1313 (2022).
6. X. Xu, G. Ren, T. Feleppa, X. Liu, A. Boes, A. Mitchell and A. J. Lowery, “Self-calibrating programmable photonic integrated circuits,”Nat. Photonics **16** (8), 595-602 (2022).
7. Y. Shen, N. C. Harris, S. Skirlo, M. Prabhu, T. Baehr-Jones, M. Hochberg, X. Sun, S. Zhao, H. Larochelle and D. Englund, “Deep learning with coherent nanophotonic circuits,”Nat. Photonics **11** (7), 441-446 (2017).
8. L. Chang, S. Liu and J. E. Bowers, “Integrated optical frequency comb technologies,”Nat. Photonics **16** (2), 95-108 (2022).
9. D. J. Moss, R. Morandotti, A. L. Gaeta and M. Lipson, “New CMOS-compatible platforms based on silicon nitride and Hydex for nonlinear optics,”Nat. Photonics **7** (8), 597-607 (2013).
10. D. Liang and J. E. Bowers, “Recent progress in lasers on silicon,”Nat. Photonics **4** (8), 511-517 (2010).
11. J. Leuthold, C. Koos and W. Freude, “Nonlinear silicon photonics,”Nat. Photonics **4** (8), 535-544 (2010).
12. K. S. Novoselov, A. K. Geim, S. V. Morozov, D.-e. Jiang, Y. Zhang, S. V. Dubonos, I. V. Grigorieva and A. A. Firsov, “Electric field effect in atomically thin carbon films,”Science **306** (5696), 666-669 (2004).
13. J. D. Caldwell, I. Aharonovich, G. Cassabois, J. H. Edgar, B. Gil and D. Basov, “Photonics with hexagonal boron nitride,”Nat. Rev. Mater. **4** (8), 552-567 (2019).
14. J. Qiao, X. Kong, Z.-X. Hu, F. Yang and W. Ji, “High-mobility transport anisotropy and linear dichroism in few-layer black phosphorus,”Nat. Commun. **5** (1), 4475 (2014).
15. C. Gu, H. Zhang, P. You, Q. Zhang, G. Luo, Q. Shen, Z. Wang and J. Hu, “Giant and multistage nonlinear optical response in porphyrin-based surface-supported metal–organic framework nanofilms,”Nano Lett. **19** (12), 9095-9101 (2019).
16. I. Abdelwahab, P. Dichtl, G. Grinblat, K. Leng, X. Chi, I. H. Park, M. P. Nielsen, R. F. Oulton, K. P. Loh and S. A. Maier, “Giant and tunable optical nonlinearity in single-crystalline 2D perovskites due to excitonic and plasma effects,”Adv. Mater. **31** (29), 1902685 (2019).
17. D. Jin, W. Liu, L. Jia, Y. Zhang, J. Hu, H. El Dirani, S. Kerdiles, C. Sciancalepore, P. Demongodin, C. Grillet, C. Monat, D. Huang, J. Wu, B. Jia and D. J. Moss, “Thickness-

and Wavelength-Dependent Nonlinear Optical Absorption in 2D Layered MXene Films,"Small Science (2024).
18. Y. Zhang, J. Wu, L. Jia, D. Jin, B. Jia, X. Hu, D. Moss and Q. Gong, "Advanced optical polarizers based on 2D materials,"npj Nanophotonics **1** (1) (2024).
19. Z. Sun, A. Martinez and F. Wang, "Optical modulators with 2D layered materials,"Nat. Photonics **10** (4), 227-238 (2016).
20. Y. Liu, N. O. Weiss, X. Duan, H.-C. Cheng, Y. Huang and X. Duan, "Van der Waals heterostructures and devices,"Nat. Rev. Mater. **1** (9), 1-17 (2016).
21. Y. Li, J. Zhang, D. Huang, H. Sun, F. Fan, J. Feng, Z. Wang and C.-Z. Ning, "Room-temperature continuous-wave lasing from monolayer molybdenum ditelluride integrated with a silicon nanobeam cavity,"Nat. Nanotechnol. **12** (10), 987-992 (2017).
22. S. Wu, S. Buckley, J. R. Schaibley, L. Feng, J. Yan, D. G. Mandrus, F. Hatami, W. Yao, J. Vučković and A. Majumdar, "Monolayer semiconductor nanocavity lasers with ultralow thresholds,"Nature **520** (7545), 69-72 (2015).
23. C. T. Phare, Y.-H. Daniel Lee, J. Cardenas and M. Lipson, "Graphene electro-optic modulator with 30 GHz bandwidth,"Nat. Photonics **9** (8), 511-514 (2015).
24. N. Flöry, P. Ma, Y. Salamin, A. Emboras, T. Taniguchi, K. Watanabe, J. Leuthold and L. Novotny, "Waveguide-integrated van der Waals heterostructure photodetector at telecom wavelengths with high speed and high responsivity,"Nat. Nanotechnol. **15** (2), 118-124 (2020).
25. H. Lin, Y. Song, Y. Huang, D. Kita, S. Deckoff-Jones, K. Wang, L. Li, J. Li, H. Zheng and Z. Luo, "Chalcogenide glass-on-graphene photonics,"Nat. Photonics **11** (12), 798-805 (2017).
26. J. Wu, Y. Yang, Y. Qu, X. Xu, Y. Liang, S. T. Chu, B. E. Little, R. Morandotti, B. Jia and D. J. Moss, "Graphene Oxide Waveguide and Micro-Ring Resonator Polarizers,"Laser Photonics Rev. **13** (9) (2019).
27. Y. Zhang, J. Wu, L. Jia, Y. Qu, Y. Yang, B. Jia and D. J. Moss, "Graphene Oxide for Nonlinear Integrated Photonics,"Laser Photonics Rev. **17** (3) (2023).
28. Q. Yang, W. Jiayang, Z. Yuning, Y. Yunyi, J. Linnan, D. Houssein El, K. Sébastien, S. Corrado, D. Pierre, G. Christian, M. Christelle, J. Baohua and J. M. David, "Integrated optical parametric amplifiers in silicon nitride waveguides incorporated with 2D graphene oxide films,"Light: Advanced Manufacturing **4** (4), 437-452 (2024).
29. V. Sorianello, M. Midrio, G. Contestabile, I. Asselberghs, J. Van Campenhout, C. Huyghebaert, I. Goykhman, A. K. Ott, A. C. Ferrari and M. Romagnoli, "Graphene–silicon phase modulators with gigahertz bandwidth,"Nat. Photonics **12** (1), 40-44 (2017).
30. Emberion to present graphene photonics developments at LASER. Optics.org https://optics.org/news/10/6/18
31. A. Montanaro, W. Wei, D. De Fazio, U. Sassi, G. Soavi, P. Aversa, A. C. Ferrari, H. Happy, P. Legagneux and E. Pallecchi, "Optoelectronic mixing with high-frequency graphene transistors,"Nat. Commun. **12** (1), 2728 (2021).
32. Swift Solar-Next generation lightweight and efficient solar technology https://www.swiftsolar.com/tech/
33. G. Jo, M. Choe, C. Y. Cho, J. H. Kim, W. Park, S. Lee, W. K. Hong, T. W. Kim, S. J. Park, B. H. Hong, Y. H. Kahng and T. Lee, "Large-scale patterned multi-layer graphene films as

transparent conducting electrodes for GaN light-emitting diodes,"Nanotechnology **21** (17), 175201 (2010).
34. Z. Wan, K. Zhang, Y. He, D. Lin, H. Dong, Y. Dong, Q. Zhang, X. Fang, X. Chen and M. Gu, "Graphene Lithography Based on Laser Reduction and Plasma Oxidization for Rewritable Hologram Imaging,"Adv. Opt. Mater. **11** (22) (2023).
35. S. Wei, G. Cao, H. Lin, X. Yuan, M. Somekh and B. Jia, "A Varifocal Graphene Metalens for Broadband Zoom Imaging Covering the Entire Visible Region,"ACS Nano **15** (3), 4769-4776 (2021).
36. X. Zheng, B. Xu, S. Li, H. Lin, L. Qiu, D. Li and B. Jia, "Free-standing graphene oxide mid-infrared polarizers,"Nanoscale **12** (21), 11480-11488 (2020).
37. T. Z. Shen, S. H. Hong and J. K. Song, "Electro-optical switching of graphene oxide liquid crystals with an extremely large Kerr coefficient,"Nat. Mater. **13** (4), 394-399 (2014).
38. Graphene for Photonics and Optoelectronics Applications | Graphene Flagship https://graphene-flagship.eu/materials/news/graphene-for-photonics-and-optoelectronics-applications/
39. About Us - Innofocus Photonics Technology https://innofocus.com.au/about-us/
40. J. Cao, D. Pavlidis, Y. Park, J. Singh and A. Eisenbach, "Improved quality GaN by growth on compliant silicon-on-insulator substrates using metalorganic chemical vapor deposition,"J. Appl. Phys. **83** (7), 3829-3834 (1998).
41. W. P. Maszara, G. Goetz, A. Caviglia and J. B. McKitterick, "Bonding of silicon wafers for silicon-on-insulator,"J. Appl. Phys. **64** (10), 4943-4950 (1988).
42. U. Helmersson, M. Lattemann, J. Bohlmark, A. P. Ehiasarian and J. T. Gudmundsson, "Ionized physical vapor deposition (IPVD): A review of technology and applications,"Thin Solid Films **513** (1), 1-24 (2006).
43. C. Elias, P. Valvin, T. Pelini, A. Summerfield, C. J. Mellor, T. S. Cheng, L. Eaves, C. T. Foxon, P. H. Beton, S. V. Novikov, B. Gil and G. Cassabois, "Direct band-gap crossover in epitaxial monolayer boron nitride,"Nat. Commun. **10** (1), 2639 (2019).
44. P. Li, W. Wei, M. Zhang, Y. Mei, P. K. Chu, X. Xie, Q. Yuan and Z. Di, "Wafer-scale growth of single-crystal graphene on vicinal Ge(001) substrate,"Nano Today **34**, 100908 (2020).
45. G. Wang, K. Wang, N. McEvoy, Z. Bai, C. P. Cullen, C. N. Murphy, J. B. McManus, J. J. Magan, C. M. Smith, G. S. Duesberg, I. Kaminer, J. Wang and W. J. Blau, "Ultrafast Carrier Dynamics and Bandgap Renormalization in Layered PtSe2,"Small **15** (34), 1902728 (2019).
46. P. Sutter, J. Lahiri, P. Zahl, B. Wang and E. Sutter, "Scalable Synthesis of Uniform Few-Layer Hexagonal Boron Nitride Dielectric Films,"Nano Lett. **13** (1), 276-281 (2013).
47. K. Y. Lin, H. W. Wan, K. H. M. Chen, Y. T. Fanchiang, W. S. Chen, Y. H. Lin, Y. T. Cheng, C. C. Chen, H. Y. Lin, L. B. Young, C. P. Cheng, T. W. Pi, J. Kwo and M. Hong, "Molecular beam epitaxy, atomic layer deposition, and multiple functions connected via ultra-high vacuum,"J. Cryst. Growth **512**, 223-229 (2019).
48. C. Elias, P. Valvin, T. Pelini, A. Summerfield, C. Mellor, T. Cheng, L. Eaves, C. Foxon, P. Beton and S. Novikov, "Direct band-gap crossover in epitaxial monolayer boron nitride,"Nat. Commun. **10** (1), 2639 (2019).
49. P. Li, W. Wei, M. Zhang, Y. Mei, P. K. Chu, X. Xie, Q. Yuan and Z. Di, "Wafer-scale

growth of single-crystal graphene on vicinal Ge (001) substrate,"Nano Today **34**, 100908 (2020).
50. D. Fu, X. Zhao, Y.-Y. Zhang, L. Li, H. Xu, A.-R. Jang, S. I. Yoon, P. Song, S. M. Poh and T. Ren, "Molecular beam epitaxy of highly crystalline monolayer molybdenum disulfide on hexagonal boron nitride,"J. Am. Chem. Soc. **139** (27), 9392-9400 (2017).
51. L. Zhang, T. Yang, X. He, W. Zhang, G. Vinai, C. S. Tang, X. Yin, P. Torelli, Y. P. Feng, P. K. J. Wong and A. T. S. Wee, "Molecular Beam Epitaxy of Two-Dimensional Vanadium-Molybdenum Diselenide Alloys,"ACS Nano **14** (9), 11140-11149 (2020).
52. W. Mortelmans, S. El Kazzi, B. Groven, A. Nalin Mehta, Y. Balaji, S. De Gendt, M. Heyns and C. Merckling, "Epitaxial registry and crystallinity of MoS2 via molecular beam and metalorganic vapor phase van der Waals epitaxy,"Appl. Phys. Lett. **117** (3) (2020).
53. W. Gao, L. Huang, J. Xu, Y. Chen, C. Zhu, Z. Nie, Y. Li, X. Wang, Z. Xie, S. Zhu, J. Xu, X. Wan, C. Zhang, Y. Xu, Y. Shi and F. Wang, "Broadband photocarrier dynamics and nonlinear absorption of PLD-grown WTe2 semimetal films,"Appl. Phys. Lett. **112** (17) (2018).
54. L. Jia, J. Wu, Y. Zhang, Y. Qu, B. Jia, Z. Chen and D. J. Moss, "Fabrication Technologies for the On-Chip Integration of 2D Materials,"Small Methods **6** (3) (2022).
55. J. D. Caldwell, T. J. Anderson, J. C. Culbertson, G. G. Jernigan, K. D. Hobart, F. J. Kub, M. J. Tadjer, J. L. Tedesco, J. K. Hite and M. A. Mastro, "Technique for the dry transfer of epitaxial graphene onto arbitrary substrates,"ACS Nano **4** (2), 1108-1114 (2010).
56. M. Liu, X. Yin, E. Ulin-Avila, B. Geng, T. Zentgraf, L. Ju, F. Wang and X. Zhang, "A graphene-based broadband optical modulator,"Nature **474** (7349), 64-67 (2011).
57. F. Xia, T. Mueller, Y.-m. Lin, A. Valdes-Garcia and P. Avouris, "Ultrafast graphene photodetector,"Nat. Nanotechnol. **4** (12), 839-843 (2009).
58. L. Cao, S. Yang, W. Gao, Z. Liu, Y. Gong, L. Ma, G. Shi, S. Lei, Y. Zhang and S. Zhang, "Direct laser-patterned micro-supercapacitors from paintable MoS2 films,"Small **9** (17), 2905-2910 (2013).
59. Y. Guo, C.-a. Di, H. Liu, J. Zheng, L. Zhang, G. Yu and Y. Liu, "General route toward patterning of graphene oxide by a combination of wettability modulation and spin-coating,"ACS Nano **4** (10), 5749-5754 (2010).
60. D. McManus, S. Vranic, F. Withers, V. Sanchez-Romaguera, M. Macucci, H. Yang, R. Sorrentino, K. Parvez, S.-K. Son and G. Iannaccone, "Water-based and biocompatible 2D crystal inks for all-inkjet-printed heterostructures,"Nat. Nanotechnol. **12** (4), 343-350 (2017).
61. J. Li, F. Ye, S. Vaziri, M. Muhammed, M. C. Lemme and M. Östling, "Efficient inkjet printing of graphene,"Adv. Mater **25** (29), 3985-3992 (2013).
62. Y. Gao, Z. Liu, D.-M. Sun, L. Huang, L.-P. Ma, L.-C. Yin, T. Ma, Z. Zhang, X.-L. Ma and L.-M. Peng, "Large-area synthesis of high-quality and uniform monolayer WS2 on reusable Au foils,"Nat. Commun. **6** (1), 8569 (2015).
63. Z.-Q. Xu, Y. Zhang, S. Lin, C. Zheng, Y. L. Zhong, X. Xia, Z. Li, P. J. Sophia, M. S. Fuhrer and Y.-B. Cheng, "Synthesis and transfer of large-area monolayer WS2 crystals: moving toward the recyclable use of sapphire substrates,"ACS Nano **9** (6), 6178-6187 (2015).
64. A. J. Watson, W. Lu, M. H. D. Guimarães and M. Stöhr, "Transfer of large-scale two-dimensional semiconductors: challenges and developments,"2D Mater. **8** (3), 032001

(2021).
65. S. Chen, G. Chen, Y. Zhao, S. Bu, Z. Hu, B. Mao, H. Wu, J. Liao, F. Li, C. Zhou, B. Guo, W. Liu, Y. Zhu, Q. Lu, J. Hu, M. Shang, Z. Shi, B. Yu, X. Zhang, Z. Zhao, K. Jia, Y. Zhang, P. Sun, Z. Liu, L. Lin and X. Wang, "Tunable Adhesion for All-Dry Transfer of 2D Materials Enabled by the Freezing of Transfer Medium,"Adv. Mater. **36** (15), e2308950 (2024).
66. Z. Lin, Y. Liu, U. Halim, M. Ding, Y. Liu, Y. Wang, C. Jia, P. Chen, X. Duan, C. Wang, F. Song, M. Li, C. Wan, Y. Huang and X. Duan, "Solution-processable 2D semiconductors for high-performance large-area electronics,"Nature **562** (7726), 254-258 (2018).
67. Y. Yang, H. Lin, B. Y. Zhang, Y. Zhang, X. Zheng, A. Yu, M. Hong and B. Jia, "Graphene-Based Multilayered Metamaterials with Phototunable Architecture for on-Chip Photonic Devices,"ACS Photonics **6** (4), 1033-1040 (2019).
68. J. Wu, L. Jia, Y. Zhang, Y. Qu, B. Jia and D. J. Moss, "Graphene Oxide for Integrated Photonics and Flat Optics,"Adv. Mater. **33** (3), e2006415 (2021).
69. Y. Yang, J. Wu, X. Xu, Y. Liang, S. T. Chu, B. E. Little, R. Morandotti, B. Jia and D. J. Moss, "Invited Article: Enhanced four-wave mixing in waveguides integrated with graphene oxide,"APL Photonics **3** (12) (2018).
70. Y. Zhang, J. Wu, Y. Yang, Y. Qu, L. Jia, T. Moein, B. Jia and D. J. Moss, "Enhanced Kerr Nonlinearity and Nonlinear Figure of Merit in Silicon Nanowires Integrated with 2D Graphene Oxide Films,"ACS Appl. Mater. Interfaces **12** (29), 33094-33103 (2020).
71. X. Gao, L. Zheng, F. Luo, J. Qian, J. Wang, M. Yan, W. Wang, Q. Wu, J. Tang, Y. Cao, C. Tan, J. Tang, M. Zhu, Y. Wang, Y. Li, L. Sun, G. Gao, J. Yin, L. Lin, Z. Liu, S. Qin and H. Peng, "Integrated wafer-scale ultra-flat graphene by gradient surface energy modulation,"Nat. Commun. **13** (1), 5410 (2022).
72. Y. Zhao, Y. Song, Z. Hu, W. Wang, Z. Chang, Y. Zhang, Q. Lu, H. Wu, J. Liao, W. Zou, X. Gao, K. Jia, L. Zhuo, J. Hu, Q. Xie, R. Zhang, X. Wang, L. Sun, F. Li, L. Zheng, M. Wang, J. Yang, B. Mao, T. Fang, F. Wang, H. Zhong, W. Liu, R. Yan, J. Yin, Y. Zhang, Y. Wei, H. Peng, L. Lin and Z. Liu, "Large-area transfer of two-dimensional materials free of cracks, contamination and wrinkles via controllable conformal contact,"Nat. Commun. **13** (1), 4409 (2022).
73. J. S. Lee, S. H. Choi, S. J. Yun, Y. I. Kim, S. Boandoh, J.-H. Park, B. G. Shin, H. Ko, S. H. Lee, Y.-M. Kim, Y. H. Lee, K. K. Kim and S. M. Kim, "Wafer-scale single-crystal hexagonal boron nitride film via self-collimated grain formation,"Science **362** (6416), 817-821 (2018).
74. M. Nakatani, S. Fukamachi, P. Solís-Fernández, S. Honda, K. Kawahara, Y. Tsuji, Y. Sumiya, M. Kuroki, K. Li, Q. Liu, Y.-C. Lin, A. Uchida, S. Oyama, H. G. Ji, K. Okada, K. Suenaga, Y. Kawano, K. Yoshizawa, A. Yasui and H. Ago, "Ready-to-transfer two-dimensional materials using tunable adhesive force tapes,"Nat. Electron. **7** (2), 119-130 (2024).
75. J. Shim, S.-H. Bae, W. Kong, D. Lee, K. Qiao, D. Nezich, Y. J. Park, R. Zhao, S. Sundaram, X. Li, H. Yeon, C. Choi, H. Kum, R. Yue, G. Zhou, Y. Ou, K. Lee, J. Moodera, X. Zhao, J.-H. Ahn, C. Hinkle, A. Ougazzaden and J. Kim, "Controlled crack propagation for atomic precision handling of wafer-scale two-dimensional materials,"Science **362** (6415), 665-670 (2018).

76. Y. Xia, X. Chen, J. Wei, S. Wang, S. Chen, S. Wu, M. Ji, Z. Sun, Z. Xu, W. Bao and P. Zhou, “12-inch growth of uniform MoS(2) monolayer for integrated circuit manufacture,”Nat. Mater. **22** (11), 1324-1331 (2023).
77. W. H. Lim, Y. K. Yap, W. Y. Chong, C. H. Pua, N. M. Huang, R. M. De La Rue and H. Ahmad, “Graphene oxide-based waveguide polariser: from thin film to quasi-bulk,”Opt. Express **22** (9), 11090-11098 (2014).
78. P. Yang, X. Zou, Z. Zhang, M. Hong, J. Shi, S. Chen, J. Shu, L. Zhao, S. Jiang, X. Zhou, Y. Huan, C. Xie, P. Gao, Q. Chen, Q. Zhang, Z. Liu and Y. Zhang, “Batch production of 6-inch uniform monolayer molybdenum disulfide catalyzed by sodium in glass,”Nat. Commun. **9** (1), 979 (2018).
79. B. Tang, H. Veluri, Y. Li, Z. G. Yu, M. Waqar, J. F. Leong, M. Sivan, E. Zamburg, Y. W. Zhang, J. Wang and A. V. Thean, “Wafer-scale solution-processed 2D material analog resistive memory array for memory-based computing,”Nat. Commun. **13** (1), 3037 (2022).
80. B. Li, Q. B. Zhu, C. Cui, C. Liu, Z. H. Wang, S. Feng, Y. Sun, H. L. Zhu, X. Su, Y. M. Zhao, H. W. Zhang, J. Yao, S. Qiu, Q. W. Li, X. M. Wang, X. H. Wang, H. M. Cheng and D. M. Sun, “Patterning of Wafer-Scale MXene Films for High-Performance Image Sensor Arrays,”Adv. Mater. **34** (17), e2201298 (2022).
81. K. Ooi, D. Ng, T. Wang, A. Chee, S. Ng, Q. Wang, L. Ang, A. Agarwal, L. Kimerling and D. Tan, “Pushing the limits of CMOS optical parametric amplifiers with USRN: Si7N3 above the two-photon absorption edge,”Nat. Commun. **8** (1), 13878 (2017).
82. M. H. Pfeiffer, A. Kordts, V. Brasch, M. Zervas, M. Geiselmann, J. D. Jost and T. J. Kippenberg, “Photonic Damascene process for integrated high-Q microresonator based nonlinear photonics,”Optica **3** (1), 20-25 (2016).
83. L. Razzari, D. Duchesne, M. Ferrera, R. Morandotti, S. Chu, B. E. Little and D. J. Moss, “CMOS-compatible integrated optical hyper-parametric oscillator,”Nat. Photonics **4** (1), 41-45 (2010).
84. S. Liu, J. Wang, J. Shao, D. Ouyang, W. Zhang, S. Liu, Y. Li and T. Zhai, “Nanopatterning Technologies of 2D Materials for Integrated Electronic and Optoelectronic Devices,”Adv. Mater. **34** (52), 2200734 (2022).
85. A. Winter, Y. Ekinci, A. Gölzhäuser and A. Turchanin, “Freestanding carbon nanomembranes and graphene monolayers nanopatterned via EUV interference lithography,”2D Mater. **6** (2), 021002 (2019).
86. P. S. Borhade, T. Chen, D. R. Chen, Y. X. Chen, Y. C. Yao, Z. L. Yen, C. H. Tsai, Y. P. Hsieh and M. Hofmann, “Self-Expansion Based Multi-Patterning for 2D Materials Fabrication beyond the Lithographical Limit,”Small **20** (22), e2311209 (2024).
87. J. Wu, Y. Yang, Y. Qu, L. Jia, Y. Zhang, X. Xu, S. T. Chu, B. E. Little, R. Morandotti, B. Jia and D. J. Moss, “2D Layered Graphene Oxide Films Integrated with Micro-Ring Resonators for Enhanced Nonlinear Optics,”Small **16** (16) (2020).
88. Y. Pak, H. Jeong, K. H. Lee, H. Song, T. Kwon, J. Park, W. Park, M. S. Jeong, T. Lee, S. Seo and G. Y. Jung, “Large-area fabrication of periodic sub-15 nm-width single-layer graphene nanorings,”Adv. Mater. **25** (2), 199-204 (2013).
89. C. Sun, J. Zhong, Z. Gan, L. Chen, C. Liang, H. Feng, Z. Sun, Z. Jiang and W.-D. Li, “Nanoimprint-induced strain engineering of two-dimensional materials,”Microsystems & Nanoengineering **10** (1), 49 (2024).

90. X. Zheng, B. Jia, H. Lin, L. Qiu, D. Li and M. Gu, “Highly efficient and ultra-broadband graphene oxide ultrathin lenses with three-dimensional subwavelength focusing,”Nat. Commun. **6**, 8433 (2015).
91. H. Lin, Z. Q. Xu, G. Cao, Y. Zhang, J. Zhou, Z. Wang, Z. Wan, Z. Liu, K. P. Loh, C. W. Qiu, Q. Bao and B. Jia, “Diffraction-limited imaging with monolayer 2D material-based ultrathin flat lenses,”Light. Sci. Appl. **9**, 137 (2020).
92. A. Enrico, O. Hartwig, N. Dominik, A. Quellmalz, K. B. Gylfason, G. S. Duesberg, F. Niklaus and G. Stemme, “Ultrafast and Resist-Free Nanopatterning of 2D Materials by Femtosecond Laser Irradiation,”ACS Nano **17** (9), 8041-8052 (2023).
93. C. Zhang, L. McKeon, M. Kremer, S. Park, O. Ronan, A. Seral-Ascaso, S. Barwich, C. Coileáin, N. McEvoy and H. Nerl, “Additive-free MXene inks and direct printing of micro-supercapacitors,”Nat. Commun. **10** (1), 1795-1795 (2019).
94. D. McManus, S. Vranic, F. Withers, V. Sanchez-Romaguera, M. Macucci, H. Yang, R. Sorrentino, K. Parvez, S. K. Son, G. Iannaccone, K. Kostarelos, G. Fiori and C. Casiraghi, “Water-based and biocompatible 2D crystal inks for all-inkjet-printed heterostructures,”Nat. Nanotechnol. **12** (4), 343-350 (2017).
95. M. G. Stanford, P. R. Pudasaini, N. Cross, K. Mahady, A. N. Hoffman, D. G. Mandrus, G. Duscher, M. F. Chisholm and P. D. Rack, “Tungsten Diselenide Patterning and Nanoribbon Formation by Gas-Assisted Focused-Helium-Ion-Beam-Induced Etching,”Small Methods **1** (4), 1600060 (2017).
96. W. Luo, W. Cai, Y. Xiang, W. Wu, B. Shi, X. Jiang, N. Zhang, M. Ren, X. Zhang and J. Xu, “In-plane electrical connectivity and near-field concentration of isolated graphene resonators realized by ion beams,”Adv. Mater. **29** (30), 1701083 (2017).
97. E. Glushkov, M. Macha, E. Rath, V. Navikas, N. Ronceray, C. Y. Cheon, A. Ahmed, A. Avsar, K. Watanabe, T. Taniguchi, I. Shorubalko, A. Kis, G. Fantner and A. Radenovic, “Engineering Optically Active Defects in Hexagonal Boron Nitride Using Focused Ion Beam and Water,”ACS Nano **16** (3), 3695-3703 (2022).
98. X. Liu, K. S. Chen, S. A. Wells, I. Balla, J. Zhu, J. D. Wood and M. C. Hersam, “Scanning Probe Nanopatterning and Layer-by-Layer Thinning of Black Phosphorus,”Adv. Mater. **29** (1) (2017).
99. Z. Wei, M. Liao, Y. Guo, J. Tang, Y. Cai, H. Chen, Q. Wang, Q. Jia, Y. Lu and Y. Zhao, “Scratching lithography for wafer-scale MoS2 monolayers,”2D Mater. **7** (4), 045028 (2020).
100. V. L. Nguyen, M. Seol, J. Kwon, E.-K. Lee, W.-J. Jang, H. W. Kim, C. Liang, J. H. Kang, J. Park, M. S. Yoo and H.-J. Shin, “Wafer-scale integration of transition metal dichalcogenide field-effect transistors using adhesion lithography,”Nat. Electron. **6** (2), 146-153 (2022).
101. Z. Wu, W. Li, M. N. Yogeesh, S. Jung, A. L. Lee, K. McNicholas, A. Briggs, S. R. Bank, M. A. Belkin and D. Akinwande, “Tunable Graphene Metasurfaces with Gradient Features by Self-Assembly-Based Moiré Nanosphere Lithography,”Adv. Opt. Mater. **4** (12), 2035-2043 (2016).
102. W. Xu and T.-W. Lee, “Recent progress in fabrication techniques of graphene nanoribbons,”Materials Horizons **3** (3), 186-207 (2016).
103. S. T. Howell, A. Grushina, F. Holzner and J. Brugger, “Thermal scanning probe

lithography—a review,”Microsystems & Nanoengineering **6** (1), 21 (2020).
104. S. Wu, S. Buckley, J. R. Schaibley, L. Feng, J. Yan, D. G. Mandrus, F. Hatami, W. Yao, J. Vučković, A. Majumdar and X. Xu, “Monolayer semiconductor nanocavity lasers with ultralow thresholds,”Nature **520** (7545), 69-72 (2015).
105. T. Tanabe, M. Notomi, S. Mitsugi, A. Shinya and E. Kuramochi, “All-optical switches on a silicon chip realized using photonic crystal nanocavities,”Appl. Phys. Lett. **87** (15) (2005).
106. V. R. Almeida, C. A. Barrios, R. R. Panepucci and M. Lipson, “All-optical control of light on a silicon chip,”Nature **431** (7012), 1081-1084 (2004).
107. T. Jiang, D. Huang, J. Cheng, X. Fan, Z. Zhang, Y. Shan, Y. Yi, Y. Dai, L. Shi, K. Liu, C. Zeng, J. Zi, J. E. Sipe, Y.-R. Shen, W.-T. Liu and S. Wu, “Gate-tunable third-order nonlinear optical response of massless Dirac fermions in graphene,”Nat. Photonics **12** (7), 430-436 (2018).
108. G. T. Reed, G. Mashanovich, F. Y. Gardes and D. J. Thomson, “Silicon optical modulators,”Nat. Photonics **4** (8), 518-526 (2010).
109. H. Arianfard, S. Juodkazis, D. J. Moss and J. Wu, “Sagnac interference in integrated photonics,”Appl. Phys. Rev. **10** (1) (2023).
110. J. Wu, P. Cao, X. Hu, X. Jiang, T. Pan, Y. Yang, C. Qiu, C. Tremblay and Y. Su, “Compact tunable silicon photonic differential-equation solver for general linear time-invariant systems,”Opt. Express **22** (21), 26254-26264 (2014).
111. J. Wu, B. Liu, J. Peng, J. Mao, X. Jiang, C. Qiu, C. Tremblay and Y. Su, “On-chip tunable second-order differential-equation solver based on a silicon photonic mode-split microresonator,”J. Lightwave Technol. **33** (17), 3542-3549 (2015).
112. R. M. Krishna, A. Eftekhar, S. Lee, T. Fan, X. Wu, A. Hosseinnia, H. Wang, M. Swaminathan and A. Adibi, “Polysilicon micro-heaters for resonance tuning in CMOS photonics,”Opt. Lett. **47** (5), 1097-1100 (2022).
113. X. Liu, P. Ying, X. Zhong, J. Xu, Y. Han, S. Yu and X. Cai, “Highly efficient thermo-optic tunable micro-ring resonator based on an LNOI platform,”Opt. Lett. **45** (22), 6318-6321 (2020).
114. Z. Wang, R. Yu, X. Wen, Y. Liu, C. Pan, W. Wu and Z. L. Wang, “Optimizing Performance of Silicon-Based p–n Junction Photodetectors by the Piezo-Phototronic Effect,”ACS Nano **8** (12), 12866-12873 (2014).
115. X. Li, H. Xu, X. Xiao, Z. Li, Y. Yu and J. Yu, “Fast and efficient silicon thermo-optic switching based on reverse breakdown of pn junction,”Opt. Lett. **39** (4), 751-753 (2014).
116. Y.-S. Duh, Y. Nagasaki, Y.-L. Tang, P.-H. Wu, H.-Y. Cheng, T.-H. Yen, H.-X. Ding, K. Nishida, I. Hotta, J.-H. Yang, Y.-P. Lo, K.-P. Chen, K. Fujita, C.-W. Chang, K.-H. Lin, J. Takahara and S.-W. Chu, “Giant photothermal nonlinearity in a single silicon nanostructure,”Nat. Commun. **11** (1), 4101 (2020).
117. Y. Shi, X. Chen, F. Lou, Y. Chen, M. Yan, L. Wosinski and M. Qiu, “All-optical switching of silicon disk resonator based on photothermal effect in metal–insulator–metal absorber,”Opt. Lett. **39** (15), 4431-4434 (2014).
118. B. Yao, S. W. Huang, Y. Liu, A. K. Vinod, C. Choi, M. Hoff, Y. Li, M. Yu, Z. Feng, D. L. Kwong, Y. Huang, Y. Rao, X. Duan and C. W. Wong, “Gate-tunable frequency combs in graphene-nitride microresonators,”Nature **558** (7710), 410-414 (2018).

119. I. Datta, S. H. Chae, G. R. Bhatt, M. A. Tadayon, B. Li, Y. Yu, C. Park, J. Park, L. Cao, D. N. Basov, J. Hone and M. Lipson, “Low-loss composite photonic platform based on 2D semiconductor monolayers,”Nat. Photonics **14** (4), 256-262 (2020).
120. G. Wu, B. Tian, L. Liu, W. Lv, S. Wu, X. Wang, Y. Chen, J. Li, Z. Wang and S. Wu, “Programmable transition metal dichalcogenide homojunctions controlled by nonvolatile ferroelectric domains,”Nat. Electron. **3** (1), 43-50 (2020).
121. Z. Shi, L. Gan, T.-H. Xiao, H.-L. Guo and Z.-Y. Li, “All-Optical Modulation of a Graphene-Cladded Silicon Photonic Crystal Cavity,”ACS Photonics **2** (11), 1513-1518 (2015).
122. L. Yu, J. Zheng, Y. Xu, D. Dai and S. He, “Local and nonlocal optically induced transparency effects in graphene–silicon hybrid nanophotonic integrated circuits,”ACS Nano **8** (11), 11386-11393 (2014).
123. J. Wu, Y. Zhang, J. Hu, Y. Yang, D. Jin, W. Liu, D. Huang, B. Jia and D. J. Moss, “2D Graphene Oxide Films Expand Functionality of Photonic Chips,”Adv. Mater., e2403659 (2024).
124. Y. K. Ryu, F. Carrascoso, R. Lopez-Nebreda, N. Agrait, R. Frisenda and A. Castellanos-Gomez, “Microheater Actuators as a Versatile Platform for Strain Engineering in 2D Materials,”Nano Lett. **20** (7), 5339-5345 (2020).
125. X. Xu, Z. O. Martin, D. Sychev, A. S. Lagutchev, Y. P. Chen, T. Taniguchi, K. Watanabe, V. M. Shalaev and A. Boltasseva, “Creating Quantum Emitters in Hexagonal Boron Nitride Deterministically on Chip-Compatible Substrates,”Nano Lett. **21** (19), 8182-8189 (2021).
126. K. Parto, S. I. Azzam, K. Banerjee and G. Moody, “Defect and strain engineering of monolayer WSe(2) enables site-controlled single-photon emission up to 150 K,”Nat. Commun. **12** (1), 3585 (2021).
127. L. Mahalingam, J. Andrews and J. Drye, “Thermal studies on pin grid array packages for high density LSI and VLSI logic circuits,”IEEE transactions on components, hybrids, and manufacturing technology **6** (3), 246-256 (1983).
128. U. R. Pfeiffer, J. Grzyb, D. Liu, B. Gaucher, T. Beukema, B. A. Floyd and S. K. Reynolds, “A chip-scale packaging technology for 60-GHz wireless chipsets,”IEEE Trans. Microwave Theory Tech. **54** (8), 3387-3397 (2006).
129. M. Wojnowski, R. Lachner, J. Böck, C. Wagner, F. Starzer, G. Sommer, K. Pressel and R. Weigel, presented at the 2011 IEEE 13th Electronics Packaging Technology Conference, 2011 (unpublished).
130. J. H. Lau, “Recent advances and trends in advanced packaging,”IEEE Transactions on Components, Packaging and Manufacturing Technology **12** (2), 228-252 (2022).
131. Photonics Packaging and Assembly-LioniX International https://www.lionix-international.com/photonics/pic-technology/assembly-and-packaging-service/
132. PHIX Characterization Package -PHIX Photonics Assembly https://www.phix.com/our-offering/prototype-package/phix-characterization-package/
133. Intel Demonstrates First Fully Integrated Optical I/O Chiplet https://www.intel.com/content/www/us/en/newsroom/news/intel-unveils-first-integrated-optical-io-chiplet.html#gs.gpexcr
134. L. Liu, P. Gong, K. Liu, A. Nie, Z. Liu, S. Yang, Y. Xu, T. Liu, Y. Zhao, L. Huang, H. Li

and T. Zhai, “Scalable Van der Waals Encapsulation by Inorganic Molecular Crystals,”Adv. Mater. **34** (7), e2106041 (2022).
135. J. Miao, L. Cai, S. Zhang, J. Nah, J. Yeom and C. Wang, “Air-Stable Humidity Sensor Using Few-Layer Black Phosphorus,”ACS Appl. Mater. Interfaces **9** (11), 10019-10026 (2017).
136. D. He, Y. Wang, Y. Huang, Y. Shi, X. Wang and X. Duan, “High-Performance Black Phosphorus Field-Effect Transistors with Long-Term Air Stability,”Nano Lett. **19** (1), 331-337 (2019).
137. F. Auksztol, D. Vella, I. Verzhbitskiy, K. F. Ng, Y. W. Ho, J. A. Grieve, J. Viana-Gomes, G. Eda and A. Ling, “Elastomeric Waveguide on-Chip Coupling of an Encapsulated MoS2 Monolayer,”ACS Photonics **6** (3), 595-599 (2019).
138. J. Jia, S. K. Jang, S. Lai, J. Xu, Y. J. Choi, J.-H. Park and S. Lee, “Plasma-treated thickness-controlled two-dimensional black phosphorus and its electronic transport properties,”ACS Nano **9** (9), 8729-8736 (2015).
139. L. Viti, D. G. Purdie, A. Lombardo, A. C. Ferrari and M. S. Vitiello, “HBN-Encapsulated, Graphene-based, Room-temperature Terahertz Receivers, with High Speed and Low Noise,”Nano Lett. **20** (5), 3169-3177 (2020).
140. IEC TR 63072-1:2017 | IEC https://webstore.iec.ch/en/publication/28046
141. ISO 10110-1:2019 - Optics and photonics - Preparation of drawings for optical elements and system shttps://www.iso.org/standard/57574.html
142. J. Hu, J. Wu, W. Liu, D. Jin, H. E. Dirani, S. Kerdiles, C. Sciancalepore, P. Demongodin, C. Grillet, C. Monat, D. Huang, B. Jia and D. J. Moss, “2D Graphene Oxide: A Versatile Thermo-Optic Material,”Adv. Funct. Mater. **n/a** (n/a), 2406799 (2024).
143. G. Ye, Y. Gong, J. Lin, B. Li, Y. He, S. T. Pantelides, W. Zhou, R. Vajtai and P. M. Ajayan, “Defects Engineered Monolayer MoS2 for Improved Hydrogen Evolution Reaction,”Nano Lett. **16** (2), 1097-1103 (2016).
144. J. R. Ferraro, *Introductory raman spectroscopy*. (Elsevier, 2003).
145. F. A. Stevie and C. L. Donley, “Introduction to x-ray photoelectron spectroscopy,”Journal of Vacuum Science & Technology A **38** (6) (2020).
146. J. Epp, in *Materials characterization using nondestructive evaluation (NDE) methods* (Elsevier, 2016), pp. 81-124.
147. H.-H. Perkampus, *UV-VIS Spectroscopy and its Applications*. (Springer Science & Business Media, 2013).
148. Y. Seo and W. Jhe, “Atomic force microscopy and spectroscopy,”Rep. Prog. Phys. **71** (1), 016101 (2007).
149. J. Mertz, *Introduction to optical microscopy*. (Cambridge University Press, 2019).
150. W. Zhou, R. Apkarian, Z. L. Wang and D. Joy, “Fundamentals of scanning electron microscopy (SEM),”Scanning microscopy for nanotechnology: techniques and applications, 1-40 (2007).
151. D. B. Williams, C. B. Carter, D. B. Williams and C. B. Carter, *The transmission electron microscope*. (Springer, 1996).
152. Y. Lin, M. Zhou, X. Tai, H. Li, X. Han and J. Yu, “Analytical transmission electron microscopy for emerging advanced materials,”Matter **4** (7), 2309-2339 (2021).
153. S. J. Pennycook and P. D. Nellist, *Scanning transmission electron microscopy: imaging*

and analysis. (Springer Science & Business Media, 2011).
154. T. H. Gfroerer, “Photoluminescence in analysis of surfaces and interfaces,”Encyclopedia of analytical chemistry **67**, 3810 (2000).
155. S. Poncé, W. Li, S. Reichardt and F. Giustino, “First-principles calculations of charge carrier mobility and conductivity in bulk semiconductors and two-dimensional materials,”Rep. Prog. Phys. **83** (3), 036501 (2020).
156. H. J. Koh, S. J. Kim, K. Maleski, S. Y. Cho, Y. J. Kim, C. W. Ahn, Y. Gogotsi and H. T. Jung, “Enhanced Selectivity of MXene Gas Sensors through Metal Ion Intercalation: In Situ X-ray Diffraction Study,”ACS Sens. **4** (5), 1365-1372 (2019).
157. Q. Lai, S. Zhu, X. Luo, M. Zou and S. Huang, “Ultraviolet-visible spectroscopy of graphene oxides,”AIP Advances **2** (3) (2012).
158. X. Zhang, C. Huang, Z. Li, J. Fu, J. Tian, Z. Ouyang, Y. Yang, X. Shao, Y. Han, Z. Qiao and H. Zeng, “Reliable wafer-scale integration of two-dimensional materials and metal electrodes with van der Waals contacts,”Nat. Commun. **15** (1), 4619 (2024).
159. E. Klugmann-Radziemska, P. Ostrowski, K. Drabczyk, P. Panek and M. Szkodo, “Experimental validation of crystalline silicon solar cells recycling by thermal and chemical methods,”Sol. Energy Mater. Sol. Cells **94** (12), 2275-2282 (2010).
160. J. Kong, D. Wei, P. Xing, X. Jin, Y. Zhuang and S. Yan, “Recycling high-purity silicon from diamond-wire saw kerf slurry waste by vacuum refining process,”Journal of Cleaner Production **286**, 124979 (2021).
161. L. Zhan, L. Jiang, Y. Zhang, B. Gao and Z. Xu, “Reduction, detoxification and recycling of solid waste by hydrothermal technology: A review,”Chem. Eng. J. **390**, 124651 (2020).
162. Q. Tao, R. Wu, Q. Li, L. Kong, Y. Chen, J. Jiang, Z. Lu, B. Li, W. Li, Z. Li, L. Liu, X. Duan, L. Liao and Y. Liu, “Reconfigurable electronics by disassembling and reassembling van der Waals heterostructures,”Nat. Commun. **12** (1), 1825 (2021).
163. T. He, Z. Wang, F. Zhong, H. Fang, P. Wang and W. Hu, “Etching Techniques in 2D Materials,”Adv. Mater. Technol. **4** (8), 1900064 (2019).
164. S. Kim, M. S. Choi, D. Qu, C. H. Ra, X. Liu, M. Kim, Y. J. Song and W. J. Yoo, “Effects of plasma treatment on surface properties of ultrathin layered MoS2,”2D Mater. **3** (3), 035002 (2016).
165. J. Van Erps, T. Ciuk, I. Pasternak, A. Krajewska, W. Strupinski, S. Van Put, G. Van Steenberge, K. Baert, H. Terryn, H. Thienpont and N. Vermeulen, “Laser ablation- and plasma etching-based patterning of graphene on silicon-on-insulator waveguides,”Opt. Express **23** (20), 26639-26650 (2015).
166. M. Zeng, Y. Xiao, J. Liu, K. Yang and L. Fu, “Exploring Two-Dimensional Materials toward the Next-Generation Circuits: From Monomer Design to Assembly Control,”Chem. Rev. **118** (13), 6236-6296 (2018).
167. D. Bol, S. Boyd and D. Dornfeld, presented at the Proceedings of the 2011 IEEE International Symposium on Sustainable Systems and Technology, 2011 (unpublished).
168. S. Kuriakose, T. Ahmed, S. Balendhran, V. Bansal, S. Sriram, M. Bhaskaran and S. Walia, “Black phosphorus: ambient degradation and strategies for protection,”2D Mater. **5** (3), 032001 (2018).
169. Q. Li, Q. Zhou, L. Shi, Q. Chen and J. Wang, “Recent advances in oxidation and degradation mechanisms of ultrathin 2D materials under ambient conditions and their

passivation strategies,”J. Mater. Chem. A **7** (9), 4291-4312 (2019).
170. A. Castellanos-Gomez, L. Vicarelli, E. Prada, J. O. Island, K. L. Narasimha-Acharya, S. I. Blanter, D. J. Groenendijk, M. Buscema, G. A. Steele, J. V. Alvarez, H. W. Zandbergen, J. J. Palacios and H. S. J. van der Zant, “Isolation and characterization of few-layer black phosphorus,”2D Mater. **1** (2), 025001 (2014).
171. Y. Huang, J. Qiao, K. He, S. Bliznakov, E. Sutter, X. Chen, D. Luo, F. Meng, D. Su and J. Decker, “Interaction of black phosphorus with oxygen and water,”Chem. Mater. **28** (22), 8330-8339 (2016).
172. X. Gan, R.-J. Shiue, Y. Gao, I. Meric, T. F. Heinz, K. Shepard, J. Hone, S. Assefa and D. Englund, “Chip-integrated ultrafast graphene photodetector with high responsivity,”Nat. Photonics **7** (11), 883-887 (2013).
173. B. Zeng, Z. Huang, A. Singh, Y. Yao, A. K. Azad, A. D. Mohite, A. J. Taylor, D. R. Smith and H.-T. Chen, “Hybrid graphene metasurfaces for high-speed mid-infrared light modulation and single-pixel imaging,”Light. Sci. Appl. **7** (1), 51 (2018).
174. K. Yao, J. D. Femi-Oyetoro, S. Yao, Y. Jiang, L. El Bouanani, D. C. Jones, P. A. Ecton, U. Philipose, M. El Bouanani, B. Rout, A. Neogi and J. M. Perez, “Rapid ambient degradation of monolayer MoS2 after heating in air,”2D Mater. **7** (1), 015024 (2019).
175. Y. Liu, B. N. Shivananju, Y. Wang, Y. Zhang, W. Yu, S. Xiao, T. Sun, W. Ma, H. Mu, S. Lin, H. Zhang, Y. Lu, C. W. Qiu, S. Li and Q. Bao, “Highly Efficient and Air-Stable Infrared Photodetector Based on 2D Layered Graphene-Black Phosphorus Heterostructure,”ACS Appl. Mater. Interfaces **9** (41), 36137-36145 (2017).
176. X. Zhao, T. Liu, Q. C. Burlingame, T. Liu, R. Holley, G. Cheng, N. Yao, F. Gao and Y.-L. Loo, “Accelerated aging of all-inorganic, interface-stabilized perovskite solar cells,”Science **377** (6603), 307-310 (2022).
177. H. H. Radamson, H. Zhu, Z. Wu, X. He, H. Lin, J. Liu, J. Xiang, Z. Kong, W. Xiong and J. Li, “State of the art and future perspectives in advanced CMOS technology,”Nanomaterials **10** (8), 1555 (2020).
178. M. Ruberti, “The chip manufacturing industry: Environmental impacts and eco-efficiency analysis,”Sci. Total Environ. **858** (Pt 2), 159873 (2023).
179. L. A. Ragnarsson, M. G. Bardon, P. Wuytens, G. Mirabelli, D. Jang, G. Willems, A. Mallik, A. Spessot, J. Ryckaert and B. Parvais, “Environmental Impact of CMOS Logic Technologies,” 82-84 (2022).
180. D. Kong, H. Wang, J. J. Cha, M. Pasta, K. J. Koski, J. Yao and Y. Cui, “Synthesis of MoS2 and MoSe2 films with vertically aligned layers,”Nano Lett. **13** (3), 1341-1347 (2013).
181. Z. Cai, B. Liu, X. Zou and H. M. Cheng, “Chemical Vapor Deposition Growth and Applications of Two-Dimensional Materials and Their Heterostructures,”Chem. Rev. **118** (13), 6091-6133 (2018).
182. M. Fojtů, W. Z. Teo and M. Pumera, “Environmental impact and potential health risks of 2D nanomaterials,”Environmental Science: Nano **4** (8), 1617-1633 (2017).
183. E. Tan, B. L. Li, K. Ariga, C. T. Lim, S. Garaj and D. T. Leong, “Toxicity of Two-Dimensional Layered Materials and Their Heterostructures,”Bioconjug. Chem. **30** (9), 2287-2299 (2019).

[184] Moss, D. J., Morandotti, R., Gaeta, A. L. & Lipson, M. “New CMOS compatible platforms based on silicon nitride and Hydex for nonlinear optics”, Nature Photonics

7, 597-607 (2013).

[185] L.Razzari, D.Duchesne, M.Ferrera, R.Morandotti, B.E Little, S.T. Chu and D.J Moss, "CMOS compatible integrated optical hyper-parametric oscillator", Nature Photonics **4** 41-44 (2010).

[186] J. S. Levy, A. Gondarenko, M. A. Foster, A. C. Turner-Foster, A. L. Gaeta, and M. Lipson, "CMOS-compatible multiple-wavelength oscillator for on-chip optical interconnects," Nature Photonics **4** 37-40 (2010).

[187] A. Pasquazi, M. Peccianti, L. Razzari, D. J. Moss, S. Coen, M. Erkintalo, Y. K. Chembo, T. Hansson, S. Wabnitz, P. DelHaye, X. Xu, A. M. Weiner, and R. Morandotti, "Micro-Combs: A Novel Generation of Optical Sources", Physics Reports **729** 1–81 (2018).

[188] T. J. Kippenberg, A. L. Gaeta, M. Lipson, and M. L. Gorodetsky, "Dissipative Kerr solitons in optical microresonators," Science **361** (2018).

[189] A. L. Gaeta, M. Lipson, and T. J. Kippenberg, "Photonic-chip-based frequency combs," Nature Photonics **13**, 158-169 (2019).

[190] Yang Sun, Jiayang Wu, Mengxi Tan, Xingyuan Xu, Yang Li, Roberto Morandotti, Arnan Mitchell, and David J. Moss, "Applications of optical micro-combs", Advances in Optics and Photonics **15** (1) 86-175 (2023).

[191] Shuman Sun, Beichen Wang, Kaikai Liu, Mark W. Harrington, Fatemehsadat Tabatabaei, Ruxuan Liu, Jiawei Wang, Samin Hanifi, Jesse S. Morgan, Mandana Jahanbozorgi, Zijiao Yang, Steven M. Bowers, Paul A. Morton, Karl D. Nelson, Andreas Beling, Daniel J. Blumenthal, and Xu Yi, "Integrated optical frequency division for microwave and mm Wave generation", Nature **627** 540 (2024).

[192] B. Corcoran, A. Mitchell, R. Morandotti, L. K. Oxenlowe, and D. J. Moss, "Microcombs for Optical Communications", Nature Photonics **18** (2024).

[193] B. Corcoran, M. Tan, X. Xu, A. Boes, J. Wu, T. G. Nguyen, S. T. Chu, B. E. Little, R. Morandotti, A. Mitchell, et al., *Nature communications* **2020**, *11*, 1 2568.

[194] P. Marin-Palomo, J. N. Kemal, M. Karpov, A. Kordts, J. Pfeifle, M. H. Pfeiffer, P. Trocha, S. Wolf, V. Brasch, M. H. Anderson, et al., *Nature* **2017**, *546*, 7657 274.

[195] D. T. Spencer, T. Drake, T. C. Briles, J. Stone, L. C. Sinclair, C. Fredrick, Q. Li, D. Westly, B. R. Ilic, A. Bluestone, et al., *Nature* **2018**, *557*, 7703 81.

[196] Kues, M. et al. "Quantum optical microcombs", Nature Photonics vol. 13, (3) 170-179 (2019).

[197] C. Reimer et al., "Generation of multiphoton entangled quantum states by means of integrated frequency combs," Science, vol. 351, no. 6278, pp. 1176-1180, 2016.

[198] M. Kues, et al., "On-chip generation of high-dimensional entangled quantum states and their coherent control", Nature, vol. 546, no. 7660, pp. 622-626, 2017.

[199] C. Reimer, et al., "High-dimensional one-way quantum processing implemented on d-

level cluster states", Nature Physics, vol. 15, no.2, pp. 148–153, 2019.

[200] X. Xu, J. Wu, T. G. Nguyen, M. Shoeiby, S. T. Chu, B. E. Little, R. Morandotti, A. Mitchell, D. J. Moss, *Optics Express* **2018**, Vol. *26*, 3 2569.

[201] J.Wu, X. Xu, T.G. Nguyen, S.T. Chu, B.E. Little, R.Morandotti, A.Mitchell, and D.J. Moss, "RF photonics: An optical micro-combs' perspective", IEEE Journal of Selected Topics in Quantum Electronics **24** (4), 1-20 Article: 6101020 (2018).

[202] M. Tan, X. Xu, J.Wu, R. Morandotti, A. Mitchell, and D. J. Moss, "RF and microwave photonic temporal signal processing with Kerr micro-combs", Advances in Physics X, VOL. 6, NO. 1, 1838946 (2021).

[203] X. Xu, M. Tan, B. Corcoran, J. Wu, A. Boes, T. G. Nguyen, S. T. Chu, B. E. Little, D. G. Hicks, R. Morandotti, et al., *Nature* **2021**, Vol. *589*, 7840 44.

[204] J. Feldmann, N. Youngblood, M. Karpov, H. Gehring, X. Li, M. Stappers, M. Le Gallo, X. Fu, A. Lukashchuk, A. S. Raja, J. Liu, C. D. Wright, A. Sebastian, T. J. Kippenberg, W. H. P. Pernice, and H. Bhaskaran, "Parallel convolutional processing using an integrated photonic tensor core", *Nature* **2021**, Vol. *589*, 7840 52.

[205] M. Tan, X. Xu, A. Boes, B. Corcoran, T. G. Nguyen, S. T. Chu, B. E. Little, R. Morandotti, J. Wu, A. Mitchell, et al., *Communications Engineering* **2023**, Vol. *2*, 1 94.

[206] B. J. Shastri, A. N. Tait, T. Ferreira de Lima, W. H. Pernice, H. Bhaskaran, C. D. Wright, P. R. Prucnal, *Nature Photonics* **2021**, *15*, 2 102.

[207] T. Herr, V. Brasch, J. D. Jost, C. Y. Wang, N. M. Kondratiev, M. L. Gorodetsky, T. J. Kippenberg, *Nature Photonics* **2014**, *8*, 2 145.

[208] M. Rowley, P.-H. Hanzard, A. Cutrona, H. Bao, S. T. Chu, B. E. Little, R. Morandotti, D. J. Moss, G.-L. Oppo, J. Sebastian T. Gongora, M. Peccianti and A. Pasquazi, "Self-emergence of robust solitons in a micro-cavity", Nature **608** (7922) 303 – 309 (2022).

[209] Hualong Bao, Andrew Cooper, Maxwell Rowley, Luigi Di Lauro, Juan Sebastian Totero Gongora, Sai T. Chu, Brent E. Little, Gian-Luca Oppo, Roberto Morandotti, David J. Moss, Benjamin Wetzel, Marco Peccianti and Alessia Pasquazi, "Laser Cavity-Soliton Micro-Combs", Nature Photonics **13** (6) 384–389 (2019).

[210] A. L. Gaeta, M. Lipson, T. J. Kippenberg, *nature photonics* **2019**, *13*, 3 158.

[211] V. Brasch, M. Geiselmann, T. Herr, G. Lihachev, M. H. Pfeiffer, M. L. Gorodetsky, T. J. Kippenberg, *Science* **2016**, *351*, 6271 357.

[212] C. Joshi, J. K. Jang, K. Luke, X. Ji, S. A. Miller, A. Klenner, Y. Okawachi, M. Lipson, A. L. Gaeta, *Optics letters* **2016**, *41*, 11 2565.

[213] H. Zhou, Y. Geng, W. Cui, S.-W. Huang, Q. Zhou, K. Qiu, C. Wei Wong, *Light: Science & Applications* **2019**, *8*, 1 50.

[214] V. Brasch, M. Geiselmann, M. H. Pfeiffer, T. J. Kippenberg, *Optics express* **2016**, *24*, 25 29312.

[215] H. Guo, M. Karpov, E. Lucas, A. Kordts, M. H. Pfeiffer, V. Brasch, G. Lihachev, V. E. Lobanov, M. L. Gorodetsky, T. J. Kippenberg, *Nature Physics* **2017**,

13, 1 94.

[216] C. Bao, L. Zhang, A. Matsko, Y. Yan, Z. Zhao, G. Xie, A. M. Agarwal, L. C. Kimerling, J. Michel, L. Maleki, et al., *Optics letters* **2014**, *39*, 21 6126.

[217] X. Xue, Y. Xuan, Y. Liu, P.-H. Wang, S. Chen, J. Wang, D. E. Leaird, M. Qi, A. M. Weiner, *Nature Photonics* **2015**, *9*, 9 594.

[218] Ó. B. Helgason, M. Girardi, Z. Ye, F. Lei, J. Schröder, V. Torres-Company, *Nature Photonics* **2023**, *17*, 11 992.

[219] A. Fülöp, M. Mazur, A. Lorences-Riesgo, Ó. B. Helgason, P.-H. Wang, Y. Xuan, D. E. Leaird, M. Qi, P. A. Andrekson, A. M. Weiner, et al., *Nature communications* **2018**, *9*, 1 1598.

[220] W. Wang, Z. Lu, W. Zhang, S. T. Chu, B. E. Little, L. Wang, X. Xie, M. Liu, Q. Yang, L. Wang, et al., *Optics letters* **2018**, *43*, 9 2002.

[221] Z. Lu, H.-J. Chen, W. Wang, L. Yao, Y. Wang, Y. Yu, B. Little, S. Chu, Q. Gong, W. Zhao, et al., *Nature communications* **2021**, *12*, 1 3179.

[222] M. Zhang, S. Ding, X. Li, K. Pu, S. Lei, M. Xiao, X. Jiang, *Nature Communications* **2024**, *15*, 1 1661.

[223] B. Y. Kim, Y. Okawachi, J. K. Jang, M. Yu, X. Ji, Y. Zhao, C. Joshi, M. Lipson, A. L. Gaeta, *Optics letters* **2019**, *44*, 18 4475.

[224] B. Shen, L. Chang, J. Liu, H. Wang, Q.-F. Yang, C. Xiang, R. N. Wang, J. He, T. Liu, W. Xie, et al., *Nature* **2020**, *582*, 7812 365.

[225] W. Jin, Q.-F. Yang, L. Chang, B. Shen, H. Wang, M. A. Leal, L. Wu, M. Gao, A. Feshali, M. Paniccia, et al., *Nature Photonics* **2021**, *15*, 5 346.

[226] H. Shu, L. Chang, Y. Tao, B. Shen, W. Xie, M. Jin, A. Netherton, Z. Tao, X. Zhang, R. Chen, et al., *Nature* **2022**, *605*, 7910 457.

[227] Q.-X. Ji, W. Jin, L. Wu, Y. Yu, Z. Yuan, W. Zhang, M. Gao, B. Li, H. Wang, C. Xiang, et al., *Optica* **2023**, *10*, 2 279.

[228] H. Weng, M. McDermott, A. A. Afridi, H. Tu, Q. Lu, W. Guo, J. F. Donegan, *Optics Express* **2024**, *32*, 3 3123.

[229] M. Karpov, M. H. Pfeiffer, H. Guo, W. Weng, J. Liu, T. J. Kippenberg, *Nature Physics* **2019**, *15*, 10 1071.

[230] M. Tan, X. Xu, Y. Li, Y. Sun, D. Hicks, R. Morandotti, J. Wu, A. Mitchell, D. J. Moss, In *Laser Resonators, Microresonators, and Beam Control XXIV*, volume 11987. SPIE, **2022** 1198702.

[231] X. Xu, M. Tan, J. Wu, T. G. Nguyen, S. T. Chu, B. E. Little, R. Morandotti, A. Mitchell, D. J. Moss, *Journal of Lightwave Technology* **2019**, Vol. *37*, 4 1288.

[232] X. Xu, M. Tan, J. Wu, A. Boes, B. Corcoran, T. G. Nguyen, S. T. Chu, B. E. Little, R. Morandotti, A. Mitchell, D. J. Moss, *IEEE Transactions on Circuits and Systems II: Express Briefs* **2020**, Vol. *67*, 12 3582.

[233] C. Mazoukh, L. Di Lauro, I. Alamgir, B. Fischer, N. Perron, A. Aadhi, A. Eshaghi,

B. E. Little, S. T. Chu, D. J. Moss, et al., *Communications Physics* **2024**, *7*, 1 81.

[234] C. E. Murray, M. Tan, C. Prayoonyong, X. Zhu, S. T. Chu, B. E. Little, R. Morandotti, A. Mitchell, D. J. Moss, B. Corcoran, Optics Express 2023, Vol. 31, 23 37749.

[235] A. Pasquazi, et al., "Sub-picosecond phase-sensitive optical pulse characterization on a chip", Nature Photonics, vol. 5, no. 10, pp. 618-623 (2011).

[236] M Ferrera et al., "On-Chip ultra-fast 1st and 2nd order CMOS compatible all-optical integration", Optics Express vol. 19 (23), 23153-23161 (2011).

[237] Bao, C., et al., Direct soliton generation in microresonators, Opt. Lett, 42, 2519 (2017).

[238] M.Ferrera et al., "CMOS compatible integrated all-optical RF spectrum analyzer", Optics Express, vol. 22, no. 18, 21488 - 21498 (2014).

[239] M. Kues, et al., "Passively modelocked laser with an ultra-narrow spectral width", Nature Photonics, vol. 11, no. 3, pp. 159, 2017.

[240] M. Ferrera, et al., "Low-power continuous-wave nonlinear optics in doped silica glass integrated waveguide structures," Nature Photonics, vol. 2, no. 12, pp. 737-740, 2008.

[241] M. Ferrera et al."On-Chip ultra-fast 1st and 2nd order CMOS compatible all-optical integration", Opt. Express, vol. 19, (23) pp. 23153-23161 (2011).

[242] D. Duchesne, M. Peccianti, M. R. E. Lamont, et al., "Supercontinuum generation in a high index doped silica glass spiral waveguide," Optics Express, vol. 18, no, 2, pp. 923-930, 2010.

[243] H Bao, L Olivieri, M Rowley, ST Chu, BE Little, R Morandotti, DJ Moss, ... "Turing patterns in a fiber laser with a nested microresonator: Robust and controllable microcomb generation", Physical Review Research vol. 2 (2), 023395 (2020).

[244] M. Ferrera, et al., "On-chip CMOS-compatible all-optical integrator", Nature Communications, vol. 1, Article 29, 2010.

[245] A. Pasquazi, et al., "All-optical wavelength conversion in an integrated ring resonator," Optics Express, vol. 18, no. 4, pp. 3858-3863, 2010.

[246] A.Pasquazi, Y. Park, J. Azana, et al., "Efficient wavelength conversion and net parametric gain via Four Wave Mixing in a high index doped silica waveguide," Optics Express, vol. 18, no. 8, pp. 7634-7641, 2010.

[247] Peccianti, M. Ferrera, L. Razzari, et al., "Subpicosecond optical pulse compression via an integrated nonlinear chirper," Optics Express, vol. 18, no. 8, pp. 7625-7633, 2010.

[248] M Ferrera, Y Park, L Razzari, BE Little, ST Chu, R Morandotti, DJ Moss, ... et al., "All-optical 1st and 2nd order integration on a chip", Optics Express vol. 19 (23), 23153-23161 (2011).

[249] M. Ferrera et al., "Low Power CW Parametric Mixing in a Low Dispersion High Index Doped Silica Glass Micro-Ring Resonator with Q-factor > 1 Million", Optics Express, vol.17, no. 16, pp. 14098–14103 (2009).

[250] M. Peccianti, et al., "Demonstration of an ultrafast nonlinear microcavity modelocked laser", Nature Communications, vol. 3, pp. 765, 2012.

[251] A.Pasquazi, et al., “Self-locked optical parametric oscillation in a CMOS compatible microring resonator: a route to robust optical frequency comb generation on a chip,” Optics Express, vol. 21, no. 11, pp. 13333-13341, 2013.

[252] A.Pasquazi, et al., “Stable, dual mode, high repetition rate mode-locked laser based on a microring resonator,” Optics Express, vol. 20, no. 24, pp. 27355-27362, 2012.

[253] H. Bao, et al., Laser cavity-soliton microcombs, Nature Photonics, vol. 13, no. 6, pp. 384-389, Jun. 2019.

[254] Antonio Cutrona, Maxwell Rowley, Debayan Das, Luana Olivieri, Luke Peters, Sai T. Chu, Brent L. Little, Roberto Morandotti, David J. Moss, Juan Sebastian Totero Gongora, Marco Peccianti, Alessia Pasquazi, “High Conversion Efficiency in Laser Cavity-Soliton Microcombs”, Optics Express Vol. 30, Issue 22, pp. 39816-39825 (2022). https://doi.org/10.1364/OE.470376.

[255] M. Rowley, P.Hanzard, A.Cutrona, H.Bao, S.Chu, B.Little, R.Morandotti, D. J. Moss, G. Oppo, J. Gongora, M. Peccianti and A. Pasquazi, “Self-emergence of robust solitons in a micro-cavity”, Nature vol. 608 (7922) 303–309 (2022).

[256] A. Cutrona, M. Rowley, A. Bendahmane, V. Cecconi,L. Peters, L. Olivieri, B. E. Little, S. T. Chu, S. Stivala, R. Morandotti, D. J. Moss, J. S. Totero-Gongora, M. Peccianti, A. Pasquazi, “Nonlocal bonding of a soliton and a blue-detuned state in a microcomb laser”, ***Nature Communications Physics*** **6** Article 259 (2023).

[257] Aadhi A. Rahim, Imtiaz Alamgir, Luigi Di Lauro, Bennet Fischer, Nicolas Perron, Pavel Dmitriev, Celine Mazoukh, Piotr Roztocki, Cristina Rimoldi, Mario Chemnitz, Armaghan Eshaghi, Evgeny A. Viktorov, Anton V. Kovalev, Brent E. Little, Sai T. Chu, David J. Moss, and Roberto Morandotti, “Mode-locked laser with multiple timescales in a microresonator-based nested cavity”, ***APL Photonics*** **9** 031302 (2024). DOI:10.1063/5.0174697.

[258] A. Cutrona, M. Rowley, A. Bendahmane, V. Cecconi,L. Peters, L. Olivieri, B. E. Little, S. T. Chu, S. Stivala, R. Morandotti, D. J. Moss, J. S. Totero-Gongora, M. Peccianti, A. Pasquazi, “Stability Properties of Laser Cavity-Solitons for Metrological Applications”, Applied Physics Letters vol. 122 (12) 121104 (2023); doi: 10.1063/5.0134147.

[259] X. Xu, J. Wu, M. Shoeiby, T. G. Nguyen, S. T. Chu, B. E. Little, R. Morandotti, A. Mitchell, and D. J. Moss, “Reconfigurable broadband microwave photonic intensity differentiator based on an integrated optical frequency comb source,” APL Photonics, vol. 2, no. 9, 096104, Sep. 2017.

[260] Xu, X., et al., Photonic microwave true time delays for phased array antennas using a 49 GHz FSR integrated micro-comb source, Photonics Research, vol. 6, B30-B36 (2018).

[261] X. Xu, M. Tan, J. Wu, R. Morandotti, A. Mitchell, and D. J. Moss, “Microcomb-based photonic RF signal processing”, IEEE Photonics Technology Letters, vol. 31 no. 23 1854-1857, 2019.

[262] Xu, et al., “Advanced adaptive photonic RF filters with 80 taps based on an integrated optical micro-comb source,” Journal of Lightwave Technology, vol. 37, no. 4, pp. 1288-1295 (2019).

[263] X. Xu, et al., “Photonic RF and microwave integrator with soliton crystal microcombs”, IEEE Transactions on Circuits and Systems II: Express Briefs, vol. 67, no. 12, pp. 3582-3586, 2020. DOI:10.1109/TCSII.2020.2995682.

[264] X. Xu, et al., “High performance RF filters via bandwidth scaling with Kerr micro-combs,” APL Photonics, vol. 4 (2) 026102. 2019.

[265] M. Tan, et al., “Microwave and RF photonic fractional Hilbert transformer based on a 50 GHz Kerr micro-comb”, Journal of Lightwave Technology, vol. 37, no. 24, pp. 6097 – 6104, 2019.

[266] M. Tan, et al., “RF and microwave fractional differentiator based on photonics”, IEEE Transactions on Circuits and Systems: Express Briefs, vol. 67, no.11, pp. 2767-2771, 2020. DOI:10.1109/TCSII.2020.2965158.

[267] M. Tan, et al., “Photonic RF arbitrary waveform generator based on a soliton crystal micro-comb source”, Journal of Lightwave Technology, vol. 38, no. 22, pp. 6221-6226 (2020). DOI: 10.1109/JLT.2020.3009655.

[268] M. Tan, X. Xu, J. Wu, R. Morandotti, A. Mitchell, and D. J. Moss, “RF and microwave high bandwidth signal processing based on Kerr Micro-combs”, Advances in Physics X, VOL. 6, NO. 1, 1838946 (2021). DOI:10.1080/23746149.2020.1838946.

[269] X. Xu, et al., “Advanced RF and microwave functions based on an integrated optical frequency comb source,” Opt. Express, vol. 26 (3) 2569 (2018).

[270] M. Tan, X. Xu, J. Wu, B. Corcoran, A. Boes, T. G. Nguyen, S. T. Chu, B. E. Little, R. Morandotti, A. Lowery, A. Mitchell, and D. J. Moss, “"Highly Versatile Broadband RF Photonic Fractional Hilbert Transformer Based on a Kerr Soliton Crystal Microcomb”, Journal of Lightwave Technology vol. 39 (24) 7581-7587 (2021).

[271] Wu, J. et al. RF Photonics: An Optical Microcombs’ Perspective. IEEE Journal of Selected Topics in Quantum Electronics Vol. 24, 6101020, 1-20 (2018).

[272] T. G. Nguyen et al., “Integrated frequency comb source-based Hilbert transformer for wideband microwave photonic phase analysis,” Opt. Express, vol. 23, no. 17, pp. 22087-22097, Aug. 2015.

[273] X. Xu, et al., “Broadband RF channelizer based on an integrated optical frequency Kerr comb source,” Journal of Lightwave Technology, vol. 36, no. 19, pp. 4519-4526, 2018.

[274] X. Xu, et al., “Continuously tunable orthogonally polarized RF optical single sideband generator based on micro-ring resonators,” Journal of Optics, vol. 20, no. 11, 115701. 2018.

[275] X. Xu, et al., “Orthogonally polarized RF optical single sideband generation and dual-channel equalization based on an integrated microring resonator,” Journal of Lightwave Technology, vol. 36, no. 20, pp. 4808-4818. 2018.

[276] X. Xu, et al., “Photonic RF phase-encoded signal generation with a microcomb source”, J. Lightwave Technology, vol. 38, no. 7, 1722-1727, 2020.

[277] X. Xu, et al., Broadband microwave frequency conversion based on an integrated optical micro-comb source”, Journal of Lightwave Technology, vol. 38 no. 2, pp. 332-338, 2020.

[278] M. Tan, et al., “Photonic RF and microwave filters based on 49GHz and 200GHz Kerr microcombs”, Optics Comm. vol. 465,125563, Feb. 22. 2020.

[279] X. Xu, et al., “Broadband photonic RF channelizer with 90 channels based on a soliton crystal microcomb”, Journal of Lightwave Technology, Vol. 38, no. 18, pp. 5116 – 5121 (2020). doi: 10.1109/JLT.2020.2997699.

[280] M. Tan et al, “Orthogonally polarized Photonic Radio Frequency single sideband generation with integrated micro-ring resonators”, IOP Journal of Semiconductors, Vol. 42 (4), 041305 (2021). DOI: 10.1088/1674-4926/42/4/041305.

[281] Mengxi Tan, X. Xu, J. Wu, T. G. Nguyen, S. T. Chu, B. E. Little, R. Morandotti, A. Mitchell, and David J. Moss, “Photonic Radio Frequency Channelizers based on Kerr Optical Micro-combs”, IOP Journal of Semiconductors Vol. 42 (4), 041302 (2021). DOI:10.1088/1674-4926/42/4/041302.

[282] B. Corcoran, et al., “Ultra-dense optical data transmission over standard fiber with a single chip source”, Nature Communications, vol. 11, Article:2568, 2020.

[283] X. Xu et al, “Photonic perceptron based on a Kerr microcomb for scalable high speed optical neural networks”, Laser and Photonics Reviews, vol. 14, no. 8, 2000070 (2020). DOI: 10.1002/lpor.202000070.

[284] Xingyuan Xu, Weiwei Han, Mengxi Tan, Yang Sun, Yang Li, Jiayang Wu, Roberto Morandotti, Arnan Mitchell, Kun Xu, and David J. Moss, “Neuromorphic computing based on wavelength-division multiplexing”, ***IEEE Journal of Selected Topics in Quantum Electronics*** **29** (2) 7400112 (2023). DOI:10.1109/JSTQE.2022.3203159.

[285] Yunping Bai, Xingyuan Xu,1, Mengxi Tan, Yang Sun, Yang Li, Jiayang Wu, Roberto Morandotti, Arnan Mitchell, Kun Xu, and David J. Moss, “Photonic multiplexing techniques for neuromorphic computing”, Nanophotonics vol. 12 (5): 795–817 (2023). DOI:10.1515/nanoph-2022-0485.

[286] Chawaphon Prayoonyong, Andreas Boes, Xingyuan Xu, Mengxi Tan, Sai T. Chu, Brent E. Little, Roberto Morandotti, Arnan Mitchell, David J. Moss, and Bill Corcoran, “Frequency comb distillation for optical superchannel transmission”, Journal of Lightwave Technology vol. 39 (23) 7383-7392 (2021). DOI: 10.1109/JLT.2021.3116614.

[287] Mengxi Tan, Xingyuan Xu, Jiayang Wu, Bill Corcoran, Andreas Boes, Thach G. Nguyen, Sai T. Chu, Brent E. Little, Roberto Morandotti, Arnan Mitchell, and David J. Moss, “Integral order photonic RF signal processors based on a soliton crystal micro-comb source”, IOP Journal of Optics vol. 23 (11) 125701 (2021). https://doi.org/10.1088/2040-8986/ac2eab

[288] Yang Sun, Jiayang Wu, Yang Li, Xingyuan Xu, Guanghui Ren, Mengxi Tan, Sai Tak Chu, Brent E. Little, Roberto Morandotti, Arnan Mitchell, and David J. Moss, “Optimizing the performance of microcomb based microwave photonic transversal signal processors”, Journal of Lightwave Technology vol. 41 (23) pp 7223-7237 (2023). DOI: 10.1109/JLT.2023.3314526.

[289] Mengxi Tan, Xingyuan Xu, Andreas Boes, Bill Corcoran, Thach G. Nguyen, Sai T. Chu, Brent E. Little, Roberto Morandotti, Jiayang Wu, Arnan Mitchell, and David J. Moss,

"Photonic signal processor for real-time video image processing based on a Kerr microcomb", Communications Engineering vol. 2 94 (2023). DOI:10.1038/s44172-023-00135-7

[290] Mengxi Tan, Xingyuan Xu, Jiayang Wu, Roberto Morandotti, Arnan Mitchell, and David J. Moss, "Photonic RF and microwave filters based on 49GHz and 200GHz Kerr microcombs", Optics Communications, vol. 465, Article: 125563 (2020). doi:10.1016/j.optcom.2020.125563. doi.org/10.1063/1.5136270.

[291] Yang Sun, Jiayang Wu, Yang Li, Mengxi Tan, Xingyuan Xu, Sai Chu, Brent Little, Roberto Morandotti, Arnan Mitchell, and David J. Moss, "Quantifying the Accuracy of Microcomb-based Photonic RF Transversal Signal Processors", IEEE Journal of Selected Topics in Quantum Electronics vol. 29 no. 6, pp. 1-17, Art no. 7500317 (2023). 10.1109/JSTQE.2023.3266276.

[292] Yang Li, Yang Sun, Jiayang Wu, Guanghui Ren, Bill Corcoran, Xingyuan Xu, Sai T. Chu, Brent. E. Little, Roberto Morandotti, Arnan Mitchell, and David J. Moss, "Processing accuracy of microcomb-based microwave photonic signal processors for different input signal waveforms", ***Photonics 10***, 10111283 (2023). DOI:10.3390/photonics10111283

[293] Yang Sun, Jiayang Wu, Yang Li, and David J. Moss, "Comparison of microcomb-based RF photonic transversal signal processors implemented with discrete components versus integrated chips", ***Micromachines* 14**, 1794 (2023). https://doi.org/10.3390/mi14091794

[294] Wu, J. et al. "2D layered graphene oxide films integrated with micro-ring resonators for enhanced nonlinear optics", Small Vol. 16, 1906563 (2020).

[295] Wu, J. et al., "Graphene oxide waveguide and micro-ring resonator polarizers", Laser and Photonics Reviews Vol. 13, 1900056 (2019).

[296] Zhang, Y. et al., "Enhanced Kerr nonlinearity and nonlinear figure of merit in silicon nanowires integrated with 2d graphene oxide films", ACS Applied Material Interfaces Vol. 12, 33094-33103 (2020).

[297] Qu, Y. et al., "Enhanced four-wave mixing in silicon nitride waveguides integrated with 2d layered graphene oxide films", Advanced Optical Materials Vol. 8, 2001048 (2020).

[298] Yuning Zhang, Jiayang Wu, Yunyi Yang, Yang Qu, Linnan Jia, Houssein El Dirani, Sébastien Kerdiles, Corrado Sciancalepore, Pierre Demongodin, Christian Grillet, Christelle Monat, Baohua Jia, and David J. Moss, "Enhanced supercontinuum generated in SiN waveguides coated with GO films", ***Advanced Materials Technologies* 8** (1) 2201796 (2023). DOI:10.1002/admt.202201796.

[299] Yuning Zhang, Jiayang Wu, Linnan Jia, Yang Qu, Baohua Jia, and David J. Moss, "Graphene oxide for nonlinear integrated photonics", ***Laser and Photonics Reviews* 17** 2200512 (2023). DOI:10.1002/lpor.202200512.

[300] Jiayang Wu, H.Lin, David J. Moss, T.K. Loh, Baohua Jia, "Graphene oxide for electronics, photonics, and optoelectronics", ***Nature Reviews Chemistry* 7** (3) 162–183 (2023). doi.org/10.1038/s41570-022-00458-7.

[301] Yang Qu, Jiayang Wu, Yuning Zhang, Yunyi Yang, Linnan Jia, Baohua Jia, and David J. Moss, "Photo thermal tuning in GO-coated integrated waveguides", Micromachines Vol. 13 1194 (2022). doi.org/10.3390/mi13081194

[302] Yuning Zhang, Jiayang Wu, Yunyi Yang, Yang Qu, Houssein El Dirani, Romain Crochemore, Corrado Sciancalepore, Pierre Demongodin, Christian Grillet, Christelle Monat, Baohua Jia, and David J. Moss, "Enhanced self-phase modulation in silicon nitride waveguides integrated with 2D graphene oxide films", IEEE Journal of Selected Topics in Quantum Electronics Vol. 29 (1) 5100413 (2023). DOI: 10.1109/JSTQE.2022.3177385

[303] Yuning Zhang, Jiayang Wu, Yunyi Yang, Yang Qu, Linnan Jia, Baohua Jia, and David J. Moss, "Enhanced spectral broadening of femtosecond optical pulses in silicon nanowires integrated with 2D graphene oxide films", Micromachines Vol. 13 756 (2022). DOI:10.3390/mi13050756.

[304] Jiayang Wu, Yuning Zhang, Junkai Hu, Yunyi Yang, Di Jin, Wenbo Liu, Duan Huang, Baohua Jia, David J. Moss, "Novel functionality with 2D graphene oxide films integrated on silicon photonic chips", ***Advanced Materials*** Vol. 36 2403659 (2024). DOI: 10.1002/adma.202403659.

[305] Di Jin, Jiayang Wu, Junkai Hu, Wenbo Liu1, Yuning Zhang, Yunyi Yang, Linnan Jia, Duan Huang, Baohua Jia, and David J. Moss, "Silicon photonic waveguide and microring resonator polarizers incorporating 2D graphene oxide films", ***Applied Physics Letters*** vol. 125, 000000 (2024); doi: 10.1063/5.0221793.

[306] Yuning Zhang, Jiayang Wu, Linnan Jia, Di Jin, Baohua Jia, Xiaoyong Hu, David Moss, Qihuang Gong, "Advanced optical polarizers based on 2D materials", ***npj Nanophotonics*** Vol. 1, (2024). DOI: 10.1038/s44310-024-00028-3.

[307] Junkai Hu, Jiayang Wu, Wenbo Liu, Di Jin, Houssein El Dirani, Sébastien Kerdiles, Corrado Sciancalepore, Pierre Demongodin, Christian Grillet, Christelle Monat, Duan Huang, Baohua Jia, and David J. Moss, "2D graphene oxide: a versatile thermo-optic material", ***Advanced Functional Materials*** **34** 2406799 (2024).

[308] Yang Qu, Jiayang Wu, Yuning Zhang, Yunyi Yang, Linnan Jia, Houssein El Dirani, Sébastien Kerdiles, Corrado Sciancalepore, Pierre Demongodin, Christian Grillet, Christelle Monat, Baohua Jia, and David J. Moss, "Integrated optical parametric amplifiers in silicon nitride waveguides incorporated with 2D graphene oxide films", ***Light: Advanced Manufacturing*** **4** 39 (2023). https://doi.org/10.37188/lam.2023.039.

[309] Di Jin, Wenbo Liu, Linnan Jia, Junkai Hu, Duan Huang, Jiayang Wu, Baohua Jia, and David J. Moss, "Thickness and Wavelength Dependent Nonlinear Optical Absorption in 2D Layered MXene Films", ***Small Science*** **4** 2400179 (2024). DOI:10.1002/smsc202400179;

[310] Linnan Jia, Jiayang Wu, Yuning Zhang, Yang Qu, Baohua Jia, Zhigang Chen, and David J. Moss, "Fabrication Technologies for the On-Chip Integration of 2D Materials", Small: Methods Vol. 6, 2101435 (2022). DOI:10.1002/smtd.202101435.

[311] Yuning Zhang, Jiayang Wu, Yang Qu, Linnan Jia, Baohua Jia, and David J. Moss, "Design and optimization of four-wave mixing in microring resonators integrated with 2D

graphene oxide films", Journal of Lightwave Technology Vol. 39 (20) 6553-6562 (2021). DOI:10.1109/JLT.2021.3101292.

[312] Yuning Zhang, Jiayang Wu, Yang Qu, Linnan Jia, Baohua Jia, and David J. Moss, "Optimizing the Kerr nonlinear optical performance of silicon waveguides integrated with 2D graphene oxide films", Journal of Lightwave Technology Vol. 39 (14) 4671-4683 (2021). DOI: 10.1109/JLT.2021.3069733.

[313] Yang Qu, Jiayang Wu, Yuning Zhang, Yao Liang, Baohua Jia, and David J. Moss, "Analysis of four-wave mixing in silicon nitride waveguides integrated with 2D layered graphene oxide films", Journal of Lightwave Technology Vol. 39 (9) 2902-2910 (2021). DOI: 10.1109/JLT.2021.3059721.

[314] Jiayang Wu, Linnan Jia, Yuning Zhang, Yang Qu, Baohua Jia, and David J. Moss, "Graphene oxide: versatile films for flat optics to nonlinear photonic chips", Advanced Materials Vol. 33 (3) 2006415, pp.1-29 (2021). DOI:10.1002/adma.202006415.

[315] Y. Qu, J. Wu, Y. Zhang, L. Jia, Y. Yang, X. Xu, S. T. Chu, B. E. Little, R. Morandotti, B. Jia, and D. J. Moss, "Graphene oxide for enhanced optical nonlinear performance in CMOS compatible integrated devices", Paper No. 11688-30, PW21O-OE109-36, 2D Photonic Materials and Devices IV, SPIE Photonics West, San Francisco CA March 6-11 (2021). doi.org/10.1117/12.2583978

[316] Yang Qu, Jiayang Wu, Yunyi Yang, Yuning Zhang, Yao Liang, Houssein El Dirani, Romain Crochemore, Pierre Demongodin, Corrado Sciancalepore, Christian Grillet, Christelle Monat, Baohua Jia, and David J. Moss, "Enhanced nonlinear four-wave mixing in silicon nitride waveguides integrated with 2D layered graphene oxide films", Advanced Optical Materials vol. 8 (21) 2001048 (2020). DOI: 10.1002/adom.202001048. arXiv:2006.14944.

[317] Yuning Zhang, Yang Qu, Jiayang Wu, Linnan Jia, Yunyi Yang, Xingyuan Xu, Baohua Jia, and David J. Moss, "Enhanced Kerr nonlinearity and nonlinear figure of merit in silicon nanowires integrated with 2D graphene oxide films", ACS Applied Materials and Interfaces vol. 12 (29) 33094−33103 (2020).

[318] Jiayang Wu, Yunyi Yang, Yang Qu, Yuning Zhang, Linnan Jia, Xingyuan Xu, Sai T. Chu, Brent E. Little, Roberto Morandotti, Baohua Jia, and David J. Moss, "Enhanced nonlinear four-wave mixing in microring resonators integrated with layered graphene oxide films", Small vol. 16 (16) 1906563 (2020). DOI: 10.1002/smll.201906563

[319] Jiayang Wu, Yunyi Yang, Yang Qu, Xingyuan Xu, Yao Liang, Sai T. Chu, Brent E. Little, Roberto Morandotti, Baohua Jia, and David J. Moss, "Graphene oxide waveguide polarizers and polarization selective micro-ring resonators", Paper 11282-29, SPIE Photonics West, San Francisco, CA, 4 - 7 February (2020). doi: 10.1117/12.2544584

[320] Jiayang Wu, Yunyi Yang, Yang Qu, Xingyuan Xu, Yao Liang, Sai T. Chu, Brent E. Little, Roberto Morandotti, Baohua Jia, and David J. Moss, "Graphene oxide waveguide polarizers and polarization selective micro-ring resonators", Laser and Photonics Reviews vol. 13 (9) 1900056 (2019). DOI:10.1002/lpor.201900056.

[321] Yunyi Yang, Jiayang Wu, Xingyuan Xu, Sai T. Chu, Brent E. Little, Roberto Morandotti, Baohua Jia, and David J. Moss, "Enhanced four-wave mixing in graphene oxide coated waveguides", Applied Physics Letters Photonics vol. 3 120803 (2018). doi: 10.1063/1.5045509.

[322] Linnan Jia, Yang Qu, Jiayang Wu, Yuning Zhang, Yunyi Yang, Baohua Jia, and David J. Moss, "Third-order optical nonlinearities of 2D materials at telecommunications wavelengths", Micromachines (MDPI), Vol. 14, 307 (2023). https://doi.org/10.3390/mi14020307.

[323] Linnan Jia, Dandan Cui, Jiayang Wu, Haifeng Feng, Tieshan Yang, Yunyi Yang, Yi Du, Weichang Hao, Baohua Jia, David J. Moss, "BiOBr nanoflakes with strong nonlinear optical properties towards hybrid integrated photonic devices", Applied Physics Letters Photonics vol. 4 090802 vol. (2019). DOI: 10.1063/1.5116621

[324] Linnan Jia, Jiayang Wu, Yunyi Yang, Yi Du, Baohua Jia, David J. Moss, "Large Third-Order Optical Kerr Nonlinearity in Nanometer-Thick PdSe2 2D Dichalcogenide Films: Implications for Nonlinear Photonic Devices", ACS Applied Nano Materials vol. 3 (7) 6876–6883 (2020). DOI:10.1021/acsanm.0c01239.

[325] Hamed Arianfard, Saulius Juodkazis, David J. Moss, and Jiayang Wu, "Sagnac interference in integrated photonics", ***Applied Physics Reviews*** **10** (1) 011309 (2023). doi: 10.1063/5.0123236.

[326] Hamed Arianfard, Jiayang Wu, Saulius Juodkazis, and David J. Moss, "Optical analogs of Rabi splitting in integrated waveguide-coupled resonators", ***Advanced Physics Research*** **2** 2200123 (2023). DOI: 10.1002/apxr.202200123.

[327] Hamed Arianfard, Jiayang Wu, Saulius Juodkazis, and David J. Moss, "Spectral shaping based on optical waveguides with advanced Sagnac loop reflectors", Paper No. PW22O-OE201-20, SPIE-Opto, Integrated Optics: Devices, Materials, and Technologies XXVI, SPIE Photonics West, San Francisco CA January 22 - 27 (2022). doi: 10.1117/12.2607902

[328] Hamed Arianfard, Jiayang Wu, Saulius Juodkazis, David J. Moss, "Spectral Shaping Based on Integrated Coupled Sagnac Loop Reflectors Formed by a Self-Coupled Wire Waveguide", IEEE Photonics Technology Letters vol. 33 (13) 680-683 (2021). DOI:10.1109/LPT.2021.3088089.

[329] Hamed Arianfard, Jiayang Wu, Saulius Juodkazis and David J. Moss, "Three Waveguide Coupled Sagnac Loop Reflectors for Advanced Spectral Engineering", Journal of Lightwave Technology vol. 39 (11) 3478-3487 (2021). DOI: 10.1109/JLT.2021.3066256.

[330] Hamed Arianfard, Jiayang Wu, Saulius Juodkazis and David J. Moss, "Advanced Multi-Functional Integrated Photonic Filters based on Coupled Sagnac Loop Reflectors", Journal of Lightwave Technology vol. 39 Issue: 5, pp.1400-1408 (2021). DOI:10.1109/JLT.2020.3037559.

[331] Hamed Arianfard, Jiayang Wu, Saulius Juodkazis and David J. Moss, "Advanced multi-functional integrated photonic filters based on coupled Sagnac loop reflectors", Paper

11691-4, PW21O-OE203-44, Silicon Photonics XVI, SPIE Photonics West, San Francisco CA March 6-11 (2021). doi.org/10.1117/12.2584020

[332] J. Wu, T. Moein, X. Xu, and D. J. Moss, "Advanced photonic filters via cascaded Sagnac loop reflector resonators in silicon-on-insulator integrated nanowires", Applied Physics Letters Photonics vol. 3 046102 (2018).

[333] J. Wu, T. Moein, X. Xu, G. Ren, A. Mitchell, and D. J. Moss, "Micro-ring resonator quality factor enhancement via an integrated Fabry-Perot cavity", Applied Physics Letters Photonics vol. 2 056103 (2017).

[334] H. Yu, S. Sciara, M. Chemnitz, N. Montaut, B. Fischer, R. Helsten, B. Crockett, B. Wetzel, T. A. Göbel, R. Krämer, B. E. Little, S. T. Chu, D. J. Moss, S. Nolte, W.J. Munro, Z. Wang, J. Azaña, R. Morandotti, "Quantum key distribution implemented with d-level time-bin entangled photons", Nature Communications Vol. 16, 171 (2025). DOI:10.1038/s41467-024-55345-0.

[335] Weiwei Han, Zhihui Liu, Yifu Xu, Mengxi Tan, Yuhua Li, Xiaotian Zhu, Yanni Ou, Feifei Yin, Roberto Morandotti, Brent E. Little, Sai Tak Chu, David J. Moss, Xingyuan Xu, and Kun Xu, "TOPS-speed complex-valued convolutional accelerator for feature extraction and inference", Nature Communications Vol. 16, 292 (2025). DOI: 10.1038/s41467-024-55321-8.

[336] Yonghang Sun, James Salamy, Caitlin E. Murray, Xiaotian Zhu, Brent E. Little, Roberto Morandotti, Arnan Mitchell, Sai T. Chu, David J. Moss, Bill Corcoran, "Self-locking of free-running DFB lasers to a single microring resonator for dense WDM", Journal of Lightwave Technology, (2024). DOI: 10.1109/JLT.2024.3494694.

[337] Zhihui Liu, Haoran Zhang, Yuhang Song, Xiaotian Zhu, Yunping Bai, Mengxi Tan, Bill Corcoran, Caitlin Murphy, Sai T. Chu, David J. Moss, Xingyuan Xu, and Kun Xu, "Advances in Soliton Crystals Microcombs", Photonics Vol. 11, 1164 (2024). https://doi.org/10.3390/photonics11121164.

[338] Di Jin, Jiayang Wu, Sian Ren, Junkai Hu, Duan Huang, and David J. Moss, "Modeling of complex integrated photonic resonators using scattering matrix method", Photonics Vol. 11, 1107 (2024). https://doi.org/10.3390/photonics11121107.

[339] Yonghang Sun, James Salamy, Caitlin E. Murry, Brent E. Little, Sai T. Chu, Roberto Morandotti, Arnan Mitchell, David J. Moss, Bill Corcoran, "Enhancing laser temperature stability by passive self-injection locking to a micro-ring resonator", Optics Express Vol. 32 (13) 23841-23855 (2024). https://doi.org/10.1364/OE.515269.

[340] C. Khallouf, V. T. Hoang, G. Fanjoux, B. Little, S. T. Chu, D. J. Moss, R. Morandotti, J. M. Dudley, B. Wetzel, and T. Sylvestre, "Raman scattering and supercontinuum generation in high-index doped silica chip waveguides", Nonlinear Optics and its Applications, edited by John M. Dudley, Anna C. Peacock, Birgit Stiller, Giovanna Tissoni, SPIE Vol. 13004, 130040I (2024). doi: 10.1117/12.3021965

[341] Yang Li, Yang Sun, Jiayang Wu, Guanghui Ren, Roberto Morandotti, Xingyuan Xu, Mengxi Tan, Arnan Mitchell, and David J. Moss, "Performance analysis of microwave

photonic spectral filters based on optical microcombs", Advanced Physics Research Vol. 3 (9) 2400084 (2024). DOI:10.1002/apxr.202400084.

[342] Di Jin, Jiayang Wu, Junkai Hu, Wenbo Liu1, Yuning Zhang, Yunyi Yang, Linnan Jia, Duan Huang, Baohua Jia, and David J. Moss, "Silicon photonic waveguide and microring resonator polarizers incorporating 2D graphene oxide films", Applied Physics Letters Vol. 125, 053101 (2024). doi: 10.1063/5.0221793.

[343] Jiayang Wu, Yuning Zhang, Junkai Hu, Yunyi Yang, Di Jin, Wenbo Liu, Duan Huang, Baohua Jia, David J. Moss, "Novel functionality with 2D graphene oxide films integrated on silicon photonic chips", Advanced Materials Vol. 36 2403659 (2024). DOI: 10.1002/adma.202403659.

[344] Yuning Zhang, Jiayang Wu, Linnan Jia, Di Jin, Baohua Jia, Xiaoyong Hu, David Moss, Qihuang Gong, "Advanced optical polarizers based on 2D materials", npj Nanophotonics 1 (2024). DOI: 10.1038/s44310-024-00028-3.

[345] Junkai Hu, Jiayang Wu, Wenbo Liu, Di Jin, Houssein El Dirani, Sébastien Kerdiles, Corrado Sciancalepore, Pierre Demongodin, Christian Grillet, Christelle Monat, Duan Huang, Baohua Jia, and David J. Moss, "2D graphene oxide: a versatile thermo-optic material", Advanced Functional Materials Vol. 34 2406799 (2024). DOI: 10.1002/adfm.202406799.

[346] Di Jin, Wenbo Liu, Linnan Jia, Junkai Hu, Duan Huang, Jiayang Wu, Baohua Jia, and David J. Moss, "Thickness and Wavelength Dependent Nonlinear Optical Absorption in 2D Layered MXene Films", Small Science Vol. 4 2400179 (2024). DOI:10.1002/smsc202400179.

[347] Andrew Cooper, Luana Olivieri, Antonio Cutrona, Debayan Das, Luke Peters, Sai Tak Chu, Brent Little, Roberto Morandotti, David J Moss, Marco Peccianti, and Alessia Pasquazi, "Parametric interaction of laser cavity-solitons with an external CW pump", Optics Express Vol. 32 (12), 21783-21794 (2024).

[348] Weiwei Han, Zhihui Liu, Yifu Xu, Mengxi Tan, Chaoran Huang, Jiayang Wu, Kun Xu, David J. Moss, and Xingyuan Xu, "Photonic RF Channelization Based on Microcombs", Special Issue on Microcombs IEEE Journal of Selected Topics in Quantum Electronics Vol. 30 (5) 7600417 (2024). DOI:10.1109/JSTQE.2024.3398419.

[349] Y. Li, Y. Sun, J. Wu, G. Ren, X. Xu, M. Tan, S. Chu, B. Little, R. Morandotti, A. Mitchell, and D. J. Moss, "Feedback control in micro-comb-based microwave photonic transversal filter systems", IEEE Journal of Selected Topics in Quantum Electronics Vol. 30 (5) 2900117 (2024). DOI: 10.1109/JSTQE.2024.3377249.

[350] Weiwei Han, Zhihui Liu, Yifu Xu, Mengxi Tan, Yuhua Li, Xiaotian Zhu, Yanni Ou, Feifei Yin, Roberto Morandotti, Brent E. Little, Sai Tak Chu, Xingyuan Xu, David J. Moss, and Kun Xu, "Dual-polarization RF Channelizer Based on Microcombs", Optics Express 32, No. 7, 11281-11295 / 25 Mar 2024 / (2024). DOI: 10.1364/OE.519235.

[351] Aadhi A. Rahim, Imtiaz Alamgir, Luigi Di Lauro, Bennet Fischer, Nicolas Perron, Pavel Dmitriev, Celine Mazoukh, Piotr Roztocki, Cristina Rimoldi, Mario Chemnitz, Armaghan Eshaghi, Evgeny A. Viktorov, Anton V. Kovalev, Brent E. Little, Sai T. Chu, David J.

Moss, and Roberto Morandotti, “Mode-locked laser with multiple timescales in a microresonator-based nested cavity”, APL Photonics Vol. 9 031302 (2024). DOI:10.1063/5.0174697.

[352] C. Mazoukh, L. Di Lauro, I. Alamgir1 B. Fischer, A. Aadhi, A. Eshaghi, B. E. Little, S. T. Chu, D. J. Moss, and R. Morandotti, “Genetic algorithm-enhanced microcomb state generation”, Nature Communications Physics Vol. 7, Article: 81 (2024) (2024). DOI: 10.1038/s42005-024-01558-0.